

Garcia, Oscar. (2020). Algorithm Development for (Near) Real Time Data Processing. (Bureau of Safety and Environmental Enforcement Oil Spill Response Research Project # 140E0120C0003).

Bureau of Safety and Environmental Enforcement Oil Spill Preparedness Division Response Research Branch Final Report

Algorithm Development for (Near) Real Time Data Processing for Oil Spill Mapping



(Photo: Water Mapping LLC, 2019)

Oscar Garcia, Diana Garcia, Francisco Haces.

Algorithm Development for (Near) Real Time Data Processing for Oil Spill Mapping

December 2021

Authors:

Oscar Garcia
Water Mapping, LLC

Diana Garcia
Water Mapping, LLC

Francisco Haces
Water Mapping, LLC

Prepared under Contract No. 140E0120C0003

By

Water Mapping, LLC
479 Deer Point Dr, Gulf Breeze, FL 32561

DISCLAIMER

Study concept, oversight, and funding were provided by the US Department of the Interior (DOI), Bureau of Safety and Environmental Enforcement (BSEE), Oil Spill Preparedness Division (OSPD), Sterling, VA, under Contract Number 140E0120C0003. This report has been technically reviewed by BSEE, and it has been approved for publication.

The views and conclusions contained in this document are those of the authors and should not be interpreted as representing the opinions or policies of the US Government, nor does mention of trade names or commercial products constitute endorsement or recommendation for use.

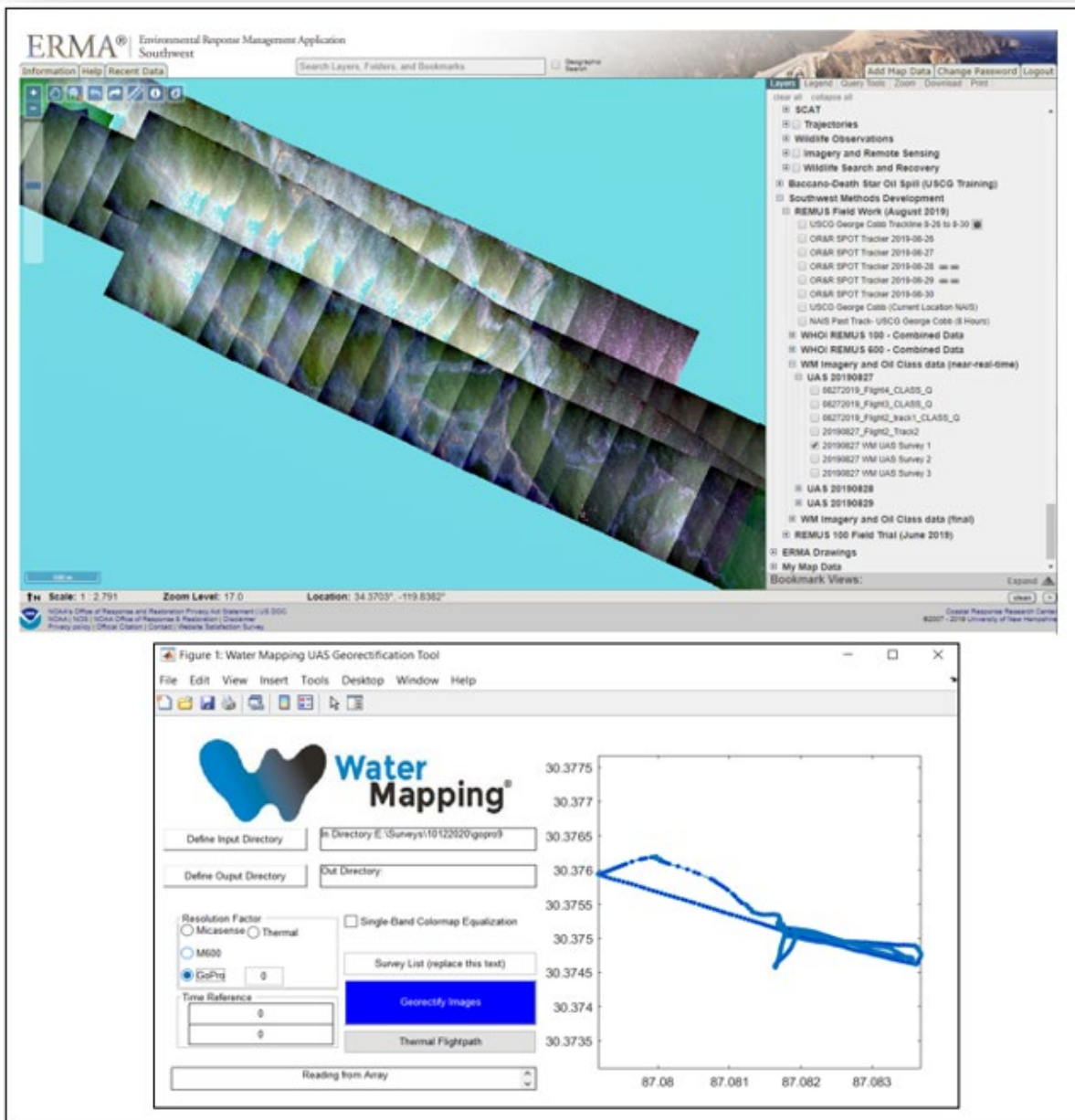
EXECUTIVE SUMMARY

With the support from the Bureau of Safety and Environmental Enforcement's (BSEE) to develop a Near and Real-time data processing algorithm for oil spill response operations support, Water Mapping, LLC (WM) has completed the three phases for this project. The ultimate goal of this project is to produce an oil spill response system in which remotely sensed images (by manned or unmanned aircrafts - UAS) are interpreted with validated algorithms, providing tactical information related to location of the oil and characteristics of the oil (thicknesses) in real and near-real time. This will help direct fleet vessels to locations where responders will have the highest remediation value. In Phase 1 of the project, WM has developed an image processing program that can be used to process data collected from any compatible aerial platforms operating a combination of Commercially available Off the Shelf (COTS) multispectral and thermal sensors. Phase 2 of the project consisted on a calibration and validation of the sensor detections based on a experiment carried out at the Cold Regions Research and Engineering Laboratory (CRREL). And lastly, the Phase 3 consisted of a series of field campaigns in which the system was tested and validated.

As a result of this work, the algorithm/sensor system is capable of identifying areas and locations of actionable oils in real-time for tactical positioning and near-real time (within under 20 minutes from being collected) for response planning. The information generated from the UAS system is compatible with The Environmental Response Management Application, (ERMA®) which will be available to responders in real and near-real time. We had the opportunity of testing this system on a real setting environment at the Santa Barbara seeps during a couple of field test in May and September of 2021. Then in October of 2021 a spill of opportunity occurred in the coast of the state of California named "Huntington Beach pipeline spill" in which we used this system to demonstrate on a real spill case the usefulness of the near real time system. During this spill we deployed our UAS system and assisted the response delivering near real time maps of the oil spill to the incident command, which helped directing the responders to the site of the detections. This successful story was later repeated as we supported an adjacent project supported by NASA producing a large number of maps of detections to support the calibration of a high altitude aerial sensor called UAVSAR.

GRAPHICAL ABSTRACT

Water Mapping UAS Georectification Tool and ERMA interface showing a collection of UAS flights that overlapped.



ABOUT THE COVER

UAS image collected by Oscar Garcia (Water Mapping, LLC) using a UAS over the Santa Barbara Seeps offshore California.

Table of Contents

List of Figures.....	vii
Abbreviations and Acronyms	viii
1 Introduction.....	1
1.1 Sensor Introduction	3
2 Phase 1. WM UAS FIGS Software	4
2.1 Software Installation	4
2.2 Launching FIGS	4
2.3 Georectification Graphical User Interface.....	5
2.4 Georectification of imagery with external flightlog and time offset.....	6
2.5 Georectification of imagery with EXIF Geotags, no external flight track	9
2.6 Georectification of imagery with no EXIF Geotags, no external flight track	12
2.7 Custom rendering defaults.....	15
3 Oil Classification	16
3.1 Supervised Classification.....	16
3.2 Example of Raster Classifications.....	17
4 Technical Documentation.....	18
4.1 Reading of File Structure.....	18
4.2 Defining an output directory	19
4.3 Selecting the appropriate sensor for the resolution factor	19
4.4 Defining Survey Lists.....	19
4.5 Theoretical basis for Georectification	20
4.6 Use of EXIF Geotagging for Georectification.....	21
4.7 Pressing the Georectify images button	23
4.8 Georectification based on UAS flightlog.....	23
4.9 Georectification without a UAS flightlog	24
4.10 Translating EXIF Geotags to images without EXIF tags	25
4.11 Reading the georectified imagery into the ArcMap Document (.mxd).....	25
4.12 Mosaicking	26
4.13 Training Samples	27
4.14 Classification	28
4.15 Prefiltering Imagery from the UAS	29
5 Phase 2: Calibration and testing of sensors.....	30
6 Phase 3. Testing of the algorithm in the field.....	40

6.1	Production of UAS orthomosaics in near real time	42
6.2	Huntington Beach Pipeline Oil Spill Incident.....	45
6.3	Oil spill monitoring during NASA-ROSES campaign.....	48
6.4	Near Real time mapping during NASA-ROSES campaign.....	51

List of Figures

Figure 1 - Previous UAS surveys collected over Santa Barbara seep 2

Figure 2 – WM FIGS Toolbar 4

Figure 3. WM Georectification GUI 5

Figure 4. Step 8 Rendering 6

Figure 5. Example Outputs – External Flightlog with Time Offset 8

Figure 6. Water Mapping UAS Georectification tool..... 9

Figure 7. Armap imagery processing..... 10

Figure 8. Example Outputs – EXIF Geotags..... 11

Figure 9. Before (left) and after (right) EXIF-geotag addition using Georectification GUI..... 13

Figure 10. Example Outputs – No EXIF Tags or External Flightlog..... 14

Figure 11. Santa Barbara flight on 08/27/20 mosaicked and projected with WM FIGS in less than 5 minutes 14

Figure 12. Classification Training Samples..... 16

Figure 13. Oil thickness classification..... 17

Figure 14. Ground view of the GRF tank with ice squares (1m x1m) and black plastic totes for oil thickness calibration. 30

Figure 15. Target thicknesses of each tote for reference of spectral and thermal reflectance..... 31

Figure 16. Aerial view of the tank setup before oil was added to the squares..... 31

Figure 17. These measurements show the maximum (red triangle), minimum (blue triangle), and average of the apparent temperatures inside the totes (Boxes 1 through 9). Flight 4 at 08:38 hr local time, overcast conditions. 33

Figure 18. Comparison of maximum, minimum, and average of apparent temperature observations for the totes vs oil thickness during Flight 4 at 8:34 AM under overcast skies and limited solar radiation..... 34

Figure 19. Apparent temperature change vs oil thickness for Flight 7 at 11:34 am under overcast skies, but with more solar radiation. 35

Figure 20. Example of difference in imagery obtained from the visual versus thermal sensors The top photo is a visual RGB image in which little can be discerned much about the variation in thickness as opposed to the apparent temperature data in the bottom image. 36

Figure 21. Thermal readings from the 24 hr time lapse of oil thicknesses for the totes. Each point is the average of apparent temperature readings every 15 minutes. 37

Figure 22. Apparent temperature readings of non-emulsified oil over a 24 hr timelapse..... 38

Figure 23. Apparent temperature of Non-Emulsified vs 50:50 Oil: Water vs 30:70 Oil: Water Emulsion... 39

Figure 24. ERMA interface showing a collection of UAS flights that overlapped..... 40

Figure 25. Orthomosaic of the oil slick with detailed zooms to appreciate the level of detail of the imagery.	42
Figure 26. WM_UAS_0511_1216Survey1, collected on May 11 at 12:16PT.....	43
Figure 27. WM_UAS_0511_1402Survey2, collected on May 11 at 14:06PT.....	43
Figure 28. WM_UAS_0511_1421Survey3, Collected on May 11 at 14:21PT	44
Figure 29. WM_UAS_0512_1354Survey7, collected on May 12 at 13:54PT.....	44
Figure 30. UAS aerial view of the oil spill from the Huntington Beach spill incident.	46
Figure 31. Near real time maps of the oil spill observed during the Huntington Beach spill.....	47
Figure 32. USCG Blackfin with its crew on deck including Ben Holt from JPL, Frank Monaldo from NOAA, and Oscar Garcia from Water Mapping, LLC.....	48
Figure 33. Thick actionable oil is observed from the UAS on October 27.	49
Figure 34. Thick actionable oil is observed from the UAS on October 28.	50
Figure 35. Thick actionable oil is observed from the UAS on October 29.	50

List of Tables

Table 1. Visual, Thermal, and Multispectral sensors used.	3
Table 2. Function of buttons on FIGS toolbar	4
Table 3. Inputs in Georectification GUI.....	5
Table 4. Example Scenarios for different kinds of stretching.....	15
Table 5. Resolution Factors for various sensors at 400 ft AGL	29

Abbreviations and Acronyms

BSEE	Bureau of Safety and Environmental Enforcement
DOI	US Department of the Interior
OSRR	Oil Spill Preparedness Division
WM	Water Mapping
GUI	Graphical User Interface
WM UAS FIGS	Water Mapping UAS Survey Fast Image Georectification System
EMS	Electromagnetic Spectrum
UAS	Unmanned Aerial System
GPS	Global Positioning System
EXIF	Exchangeable Image File Format
RGB	Red, Blue, and Green
FLIR	Forward-Looking InfraRed
COTS	Commercial Out of The Shelf
USCG	United States Coast Guard

1 Introduction

The Water Mapping UAS Survey Fast Image Georectification System (WM UAS FIGS) produces operational information for field workers in response to an oil spill. In particular, UAS FIGS enables the operators to orthorectify, mosaic, and classify snapshots collected during a survey, which can then be used to coordinate response operations and to provide stakeholders with valuable, time-sensitive information. This system is composed of two subroutines: a MATLAB-based georectification algorithm and an ArcMap-based mosaic and classification workflow. As such, the toolbar requires the following software packages to be installed in a workstation or mobile laptop where the system will be used:

- MATLAB (2019a or later) with Mapping Toolbox
- ArcMap 10.5 with ArcPy installation
- Python 3.6 or later

An Unmanned Aerial System (UAS), colloquially known as drone, collects data using downward-facing sensors while operated by a UAS pilot. The sensors collect sequentially-timed snapshots of the surface directly below the flightpath. A sensor can be facing the navigation direction (nadir), or can be placed at an angle within the UAS to collect side-viewing imagery (oblique). When the angle of the sensor within the UAS is close to perpendicular to the ground, vertical imagery is obtained, contrasted to the oblique imagery collected by side-viewing sensors. Although a snapshot of the sensor imagery is transmitted via radio signal to the pilot for navigation purposes, the collected imagery can be recorded by the sensor's mounted storage unit. Imagery is saved with EXIF metadata, which can contain geotagging information depending on the sensor. When several images are collected with EXIF geotags, a collection of multiple snapshots over the flight track can be constructed, which can then be used to orthorectify imagery in a geospatial projection, this process is known as mosaicking stills and this is what we will be using for providing with a rapid georectification mechanism.

There are several Commercial Out of The Shelf (COTS) sensors which can be mounted in a UAS. Since sensors generally collect data on certain portions (or bands) of the electromagnetic spectrum (EMS), COTS are often named according to the sections of the EMS they record. For example, a visual sensor should collect data on the Red, Green, and Blue bands (RGB), and as such is referred to as an RGB sensor. A Forward-Looking InfraRed (FLIR) sensor will collect a band within the thermal infrared section of the EMS. A multispectral sensor will often collect bands across several portions of the EMS. Because different targets respond differently to each band of the EMS, imaging with multiple sensors allows for the distinction between different targets, such as vegetation and built structures, or in the case of this toolbar, floating oil of various thicknesses and water. For the Phase-1 of this project we used previous UAS surveys collected over spill sites and new UAS surveys collected over shorelines.



Figure 1 - Previous UAS surveys collected over Santa Barbara seep sites are used on the development of this software. In this image we show a UAS take off from a USCG vessel. The aircraft has a flight time duration of up to 35 minutes and its rigged with a high resolution dual Thermal and Visual camera.






1.1 Sensor Introduction

For the purposes of the development of WM UAS FIGS, three sensors were validated for use for the detection of floating oil. These are an RGB sensor, a FLIR sensor, and a multispectral sensor. The features of each of these are described in the paragraphs below.

- **RGB Sensors:** These sensors collect the bands in the EMS which are visible to humans. Beyond allowing for clear navigation, the RGB sensor can distinguish between rainbow sheens, thick darks, and open water through the combination of the red, green, and blue bands. Two RGB sensors were used, a GoPro sensor and an M600 sensor.
- **FLIR Sensor:** This sensor collects data on the thermal infrared band of the EMS, and can be used to detect temperature differences between spilled oil and open water.
- **Multispectral Sensor:** This is a Micasense Multispectral sensor which collects data across five different spectral bands. These include a Blue, Green, Red, RedEdge, and Near Infrared band, which jointly allow for a wider gamut of data for classification techniques.

The specific sensor packages used during this project are:

Table 1. Visual, Thermal, and Multispectral sensors used.

Dual Visual/Thermal Model Flir Vue Duo Pro R	Thermal Flir Vue Pro	Multispectral Micasense Rededge	Dual Visual/Thermal Model Flir XT2	Multispectral H20T
				

Links for full specs of these sensor are:

<https://www.flir.com/support/products/duo-pro-r/#Overview>

<https://www.flir.com/products/vue-pro-r/>

<https://micasense.com/rededge-mx/>

<https://www.dji.com/zenmuse-h20-series>

<https://www.flir.com/products/xt2/>

2 Phase 1. WM UAS FIGS Software

2.1 Software Installation

The installation of the WM UAS FIGS on a workstation requires configuration of multiple libraries for the operating system (e.g. Windows 10) and the software packages (Matlab, Python, Arcmap), as this requires special modifications of script locations and installers, as well as limited modification of the scripts themselves. After installation, a new quick access icon should be seen on the desktop (which will run on the background Matlab) and a new toolbar will be available within the ArcMap installation of the workstation. These two-software combined (Matlab GUI and Arcmap toolbar) will enable the processing of UAS snapshots into actionable products.

2.2 Launching FIGS

To launch the program, the WaterMapping FIGS georectification toolbar must be activated within ArcMap. This toolbar contains the launcher for the MATLAB-based script, as well as the required ArcPy-based tools to generate the mosaics and classifications. This toolbar is shown in Figure 1. Table 1 shows the function of each of the inputs of the toolbar.



Figure 2 – WM FIGS Toolbar

Table 2 – Function of buttons on FIGS toolbar

Function	Description
Launch GUI	Launches a MATLAB command prompt and the Georectification GUI.
Read files	Reads file structure of location where current map document is saved. Each folder is added as a separate group, and .lyr files are created for rasters which do not have one already.
Skip Dropdown	Changes visibility in every 0, 1, 2, or 3 layers to improve cross-image boundary for slow moving flights. Default is 0.
Fast Export	Will iterate through each group layer, zoom to extent, and then take a screenshot of the layout, saving it to AAA_Mosaic within the output folder. The side length of the screenshot is defined as the selection on the Out Resolution dropdown, in pixels.
Out resolution	Will modify the fast export resolution. Default is 3000.
Quality Export	Uses Mosaic to New Raster tool to generate a high-resolution mosaic from the images in each group layer.

2.3 Georectification Graphical User Interface

The georectification algorithm can be launched by pressing the “Launch GUI” button on the WM Georectification Toolbar within ArcMap. This will start a MATLAB command prompt, which will subsequently launch the WM Georectification Graphical User Interface (GUI). The GUI is presented in Figure 2. Each of the inputs to the GUI, and their corresponding functions, are explained in Table 2.

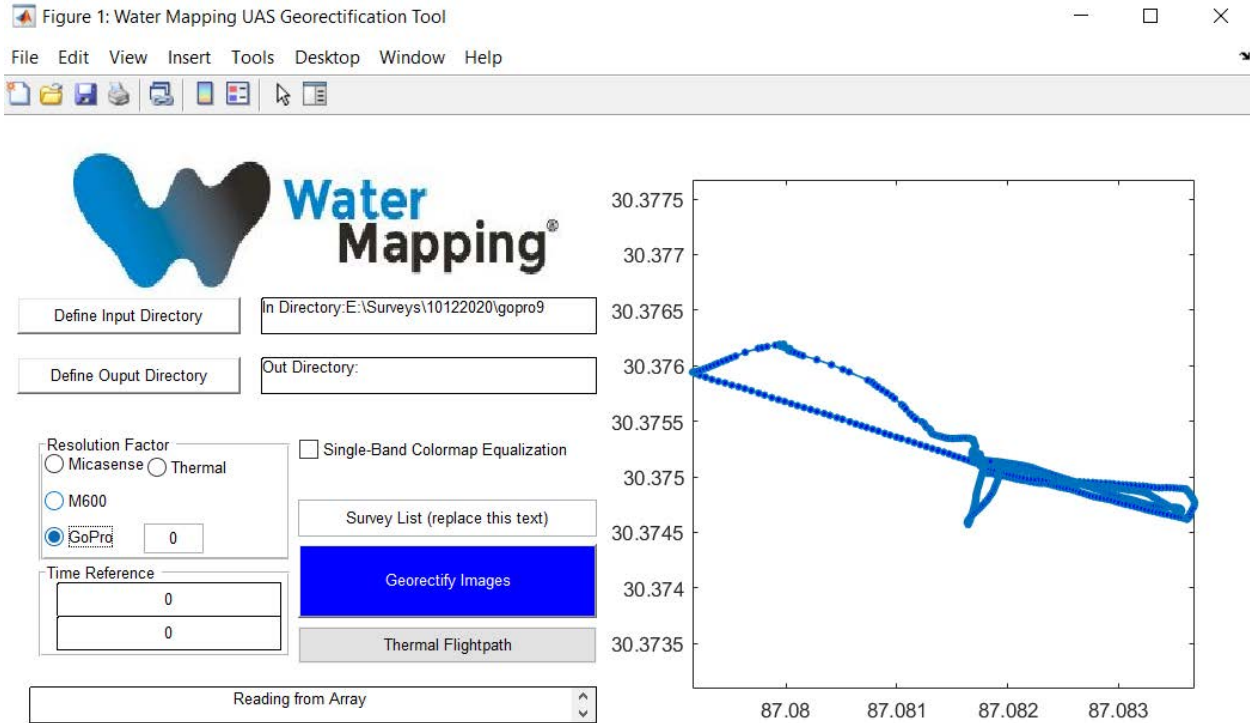


Figure 3. WM Georectification GUI

Table 3. Inputs in Georectification GUI

Input	Description
Define Input Directory	Launches a File Explorer window to define the folder with all the UAS snapshots to be processed. This function crawls through the subfolders in the selected directory searching for JPG and TIF snapshots. After finishing the crawling process, the image geotags are plot on the right.
Define Output Directory	Launches a File Explorer window to define the folder where all the exported snapshots, with their corresponding world files (EG, .tfw or .jpw), should be saved. To simplify operations, and enable the fast georectification of surveys from multiple sensors, an output folder with the run date and time are created within the selected folder To enable the distinction between different sensors, the output is saved within a file structure readable by the ArcPy functions within the WM FIGS toolbar.
Resolution Factor	Defines the scaling factor used to project rasters to the Web Mercator coordinate system. This is closely related to the flight altitude. The appropriate sensor for a given run should be selected in this input.

	The selection of a given sensor projects the snapshots assuming a 400 ft flight altitude. Should a different altitude be used, the textbox enables users to customize resolution factors. The text box input will only be used for resolution factor if it is not equal to 0, and it is not empty.
Time Reference	In cases where a flight track was provided, the first textbox functions as the reference image, while the second corresponds to the “real time” during that image. This allows for a time correction of the EXIF data of the images, in particular of the timestamp, to properly place within the georectification map.
Single-Band Colormap Equalization	If checked, will assign the pixel at location (1,1) a value of 254, and at (1,2) a value of 0 for all bands. This helps all images to be shown similarly within a GIS environment. Will only work for 8 bit images
Survey List	Search strings for confinement of exported materials. In surveys with thousands of snapshots, processing can take very long to export. As such, this is offered as a constraining tool to ensure that only certain images are included in the processing. For example, if only images IMG_002 to IMG_008 and IMG_012 to IMG_040 were of interest, this textbox could be used by inputting “2-8,12-40” to limit the processing to just those images.
Georectify Images	After all the inputs have been filled, this button starts the georectification process.
Thermal Flightpath	Launches a secondary window to permit the writing of EXIF tags to images without geotags.
Status	Status bar. Monitor this along with the MATLAB command window to see the status of the run.

2.4 Georectification of imagery with external flightlog and time offset

1. Launch ArcMap and select “Launch GUI” on the WM UAS FIGS toolbar. Wait for MATLAB command prompt and GUI to appear.
2. Extract flighttrack from UAS and place CSV in same location as imagery, or imagery subfolders
3. Select input folder, with the imagery collected by sensor and flighttrack (Step 2). Wait for flight track plot to appear on right.
4. Select output folder to save outputs.
5. Define appropriate resolution factor (only use radio button if flight was at 400 ft).
6. Examine first image of survey with time reference. In the first textbox under Time Reference, type the image name (EG, “IMG_0001”). In the second, type the 24hr-formatted time reference within the image (EG, “13:23:40”).
7. (OPTIONAL) Use plot to select which images to export, and add to survey list in following format:
XXXXX-XXXXX,XXXXX-XXXXX,XXXXX-XXXXX

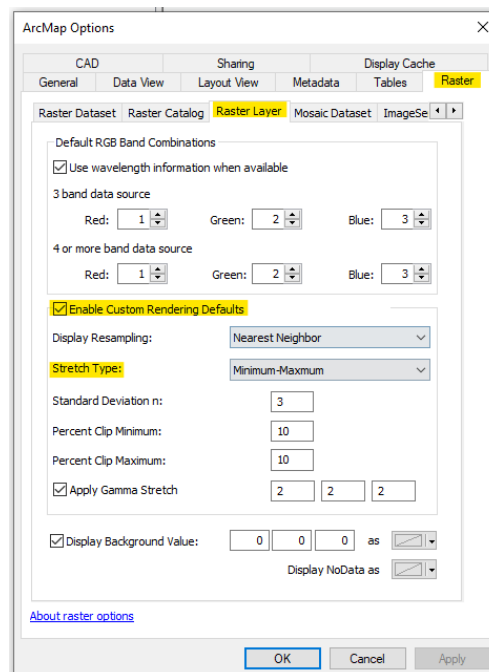


Figure 4. Step 8 Rendering

8. Select Georectify button, and monitor MATLAB command prompt with status bar. Wait until File Explorer window with export directory opens.
9. Return to ArcMap, and Save Document in the directory returned in Step 6.
10. In ArcMap, select Customize, ArcMap options. Under Raster Menu, select Raster Layer, and Enable Custom Rendering Defaults (see figure on the right). Change stretch type to desired stretching (See Custom Rendering Defaults section for further discussion on this step). Click OK.
11. Select Read Files and wait for ArcMap to finish adding processed imagery.
12. (OPTIONAL) Select an appropriate Skip step.
13. Examine imagery, and turn off or remove undesired images
14. Select Fast Export and wait for fast mosaic rasters to be added to Map Document.

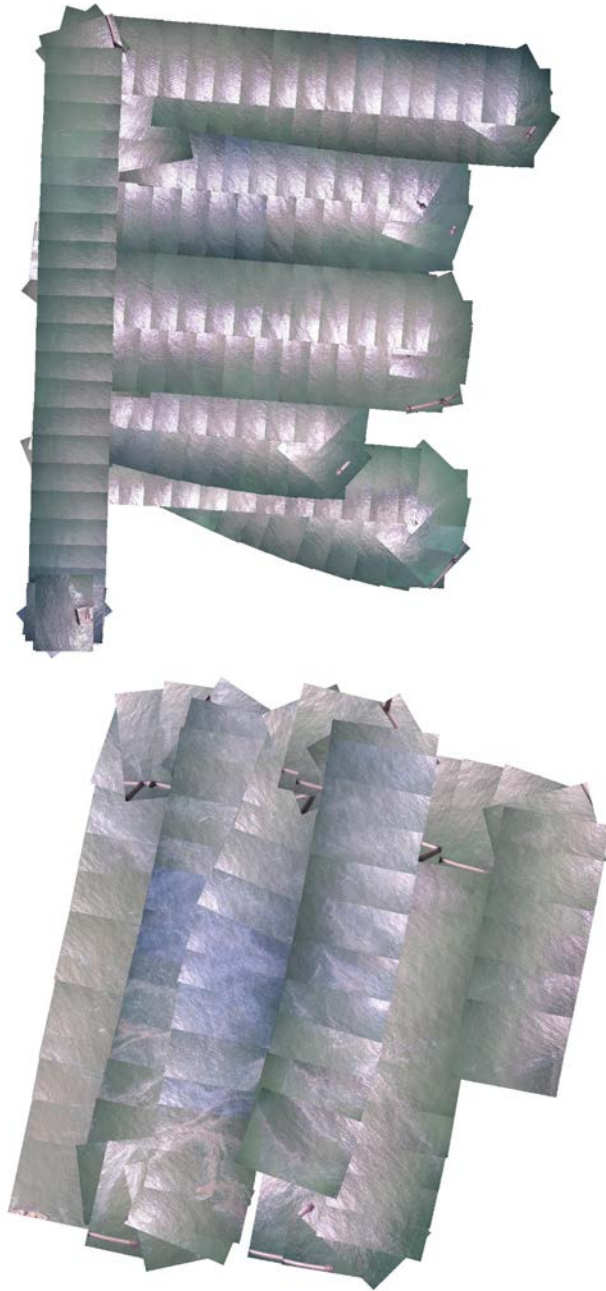


Figure 5. Example Outputs – External Flightlog with Time Offset

To demonstrate the performance of the WM-FIGS software we use examples from surveys of data collected from past missions. The examples above show two Santa Barbara flights on 08/29/2019. These mosaic outputs (Without Classification) can be obtained in less than 10 minutes of processing.

2.5 Georectification of imagery with EXIF Geotags, no external flight track

1. Launch ArcMap and select “Launch GUI” on the WM UAS FIGS toolbar. Wait for MATLAB command prompt and GUI to appear.
2. Select input folder, with the imagery collected by sensor. Wait for flight track plot to appear on right.
3. Select output folder to save outputs
4. Define appropriate resolution factor (only use radio button if flight was at 400 ft).
5. (OPTIONAL) Use plot to select which images to export, and add to survey list in following format: XXXXX-XXXXX,XXXXX-XXXXX,XXXXX-XXXXX (see figure below).

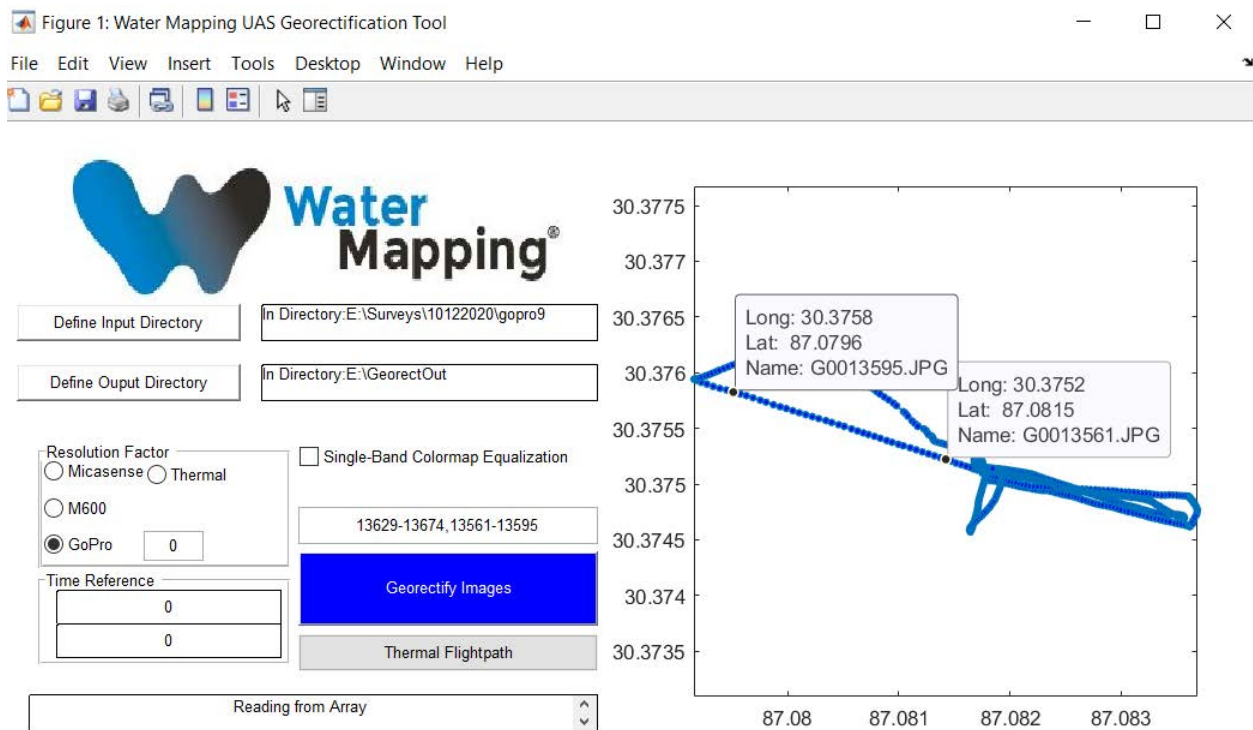


Figure 6 – Water Mapping UAS Georectification tool

6. Select Georectify button, and monitor MATLAB command prompt with status bar. Wait until File Explorer window with export directory opens.
7. Return to ArcMap, and Save Document in the directory returned in Step 6.
8. In ArcMap, select Customize, ArcMap options. Under Raster Menu, select Raster Layer, and Enable Custom Rendering Defaults (see figure on the right). Change stretch type to desired stretching (See the custom rendering defaults section for a deeper discussion of this step). Click OK.
9. Select Read Files and wait for ArcMap to finish adding processed imagery.

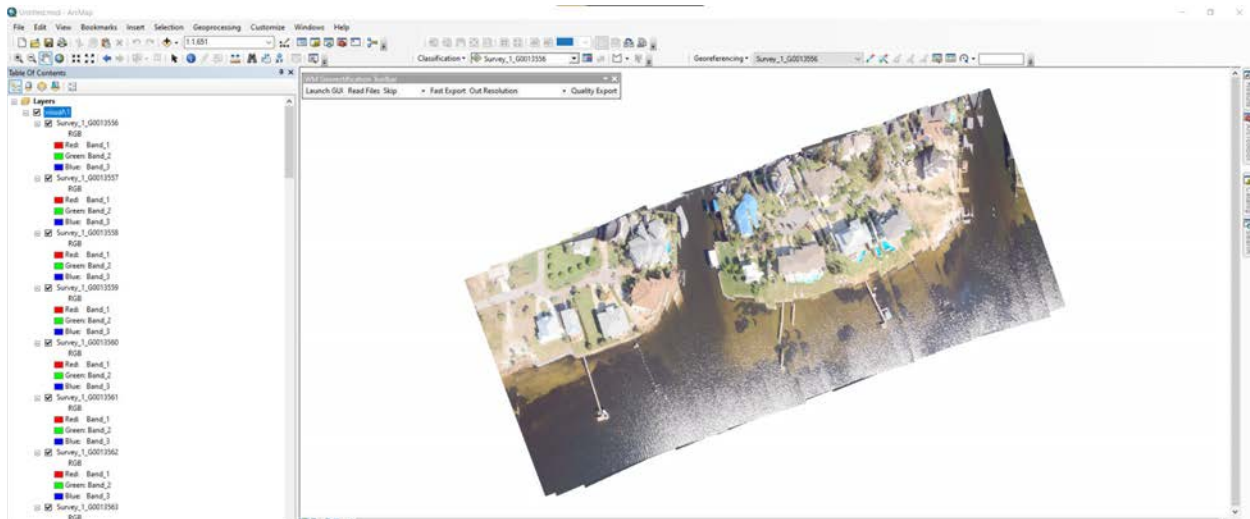


Figure 7. Armap imagery processing

10. (OPTIONAL) Select an appropriate Skip step.
11. Examine imagery, and turn off or remove undesired images
12. Select Fast Export and wait for fast mosaic rasters to be added to Map Document.



Figure 8. Example Outputs – EXIF Geotags

In order to test accuracy and processing speed of the software, we conducted multiple flights on shorelines. The example above shows a residential community in Florida where flights were conducted at different altitudes. The clarity on this example demonstrate the accuracy on the alignment of the georectification. Even though is not perfect and there could be seen some misalignments on the shoreline, the offset of less than 10ft within stills is acceptable for the rapid projection of the mosaics in less than 10 minutes of processing. Flight flown on 05/10/2020.

2.6 Georectification of imagery with no EXIF Geotags, no external flight track

1. Perform georectification of imagery with EXIF Geotags (See SOP – Georectification of Imagery with EXIF Geotags).
2. Identify “timeseries.csv” within output folder from Step 1.
3. If necessary, select Launch GUI from WM UAS FIGS toolbar.
4. Select “Thermal Flightpath” within the Georectification GUI.
5. Replace “Input the non-EXIF directory” with the directory where the Non-EXIF imagery is (EG, “D:\non_exif_data”).
6. Replace “Input timeseries path (including filename)” with the file path to the “timeseries.csv” file identified in Step 2 (EG, “D:\exif_data\20-Oct-2020_09-39-24\timeseries.csv”).
7. Replace “Input offset from UTC (regular: -7:00:00)” with a desired offset from UTC. Central Standard Time would require “-7:00:00” to be input.
 - a. This field can also be used to fix an offset caused by a time discrepancy between the two sensors. If the EXIF sensor is 30 seconds ahead of the non-EXIF sensor, this could be input as “-6:59:30”.
8. Select Fixem and monitor MATLAB command prompt. After verbose output stops and when prompted, press enter on command prompt to finish EXIF interpolation.
9. Open a file explorer window and examine properties of imagery to ensure that files now have EXIF geotags (See figure 4). If no geotags are found, see troubleshooting steps in section XX.
10. Select input folder (same directory as Step 5). Wait for flight track plot to appear on right.
11. Select output folder to save georectified outputs.
12. Define appropriate resolution factor (only use radio button if flight was at 400 ft).
13. (OPTIONAL) Use plot to select which images to export, and add to survey list in following format: XXXXX-XXXXX,XXXXX-XXXXX,XXXXX-XXXXX
14. Select Georectify button, and monitor MATLAB command prompt with status bar. Wait until File Explorer window with export directory opens.
15. Return to ArcMap, and Save Document in the directory returned in Step 6.
16. In ArcMap, select Customize, ArcMap options. Under Raster Menu, select Raster Layer, and Enable Custom Rendering Defaults (see figure on the right). Change stretch type to desired stretching (See section XX for a deeper discussion on this step). Click OK.
17. Select Read Files and wait for ArcMap to finish adding processed imagery.
18. (OPTIONAL) Select an appropriate Skip step.
19. Examine imagery, and turn off or remove undesired images
20. Select Fast Export and wait for fast mosaic rasters to be added to Map Document.

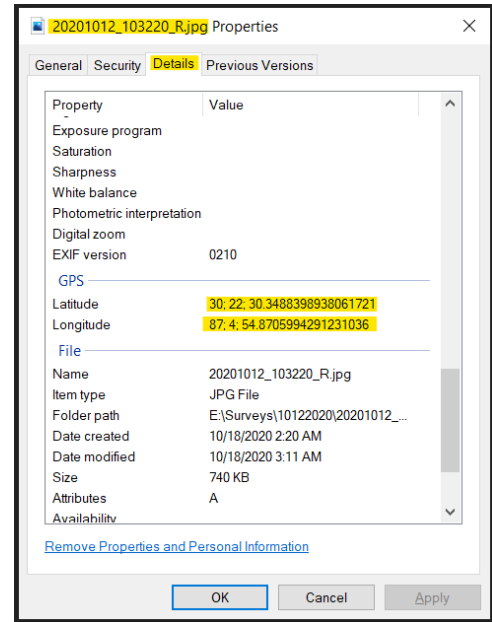
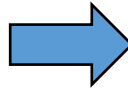
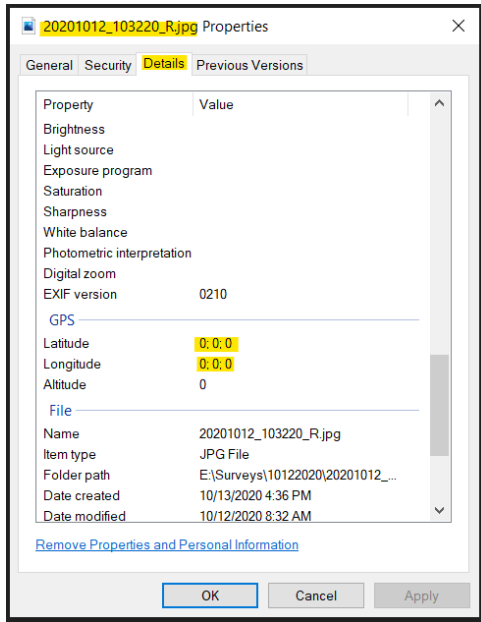
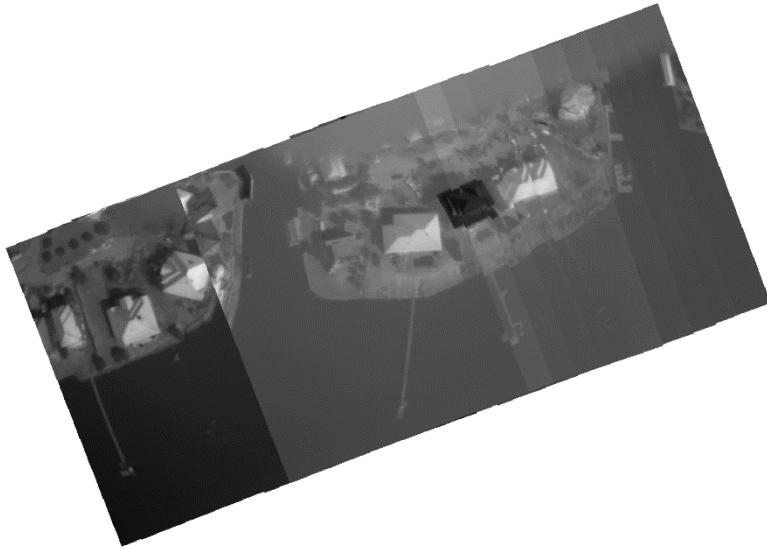


Figure 9. Before (left) and after (right) EXIF-geotag addition using Georectification GUI.



This example shows the rapid projection of imagery without GPS EXIF information. This example shows several artifacts and misalignments, however the fact that extra sensors (without GPS) can be georeferenced with our WM FIGS software is a great advantage and opens up possibility for inclusion of many more sensors. Flight flown on 06/17/2020.

Figure 10. Example Outputs – No EXIF Tags or External Flightlog.

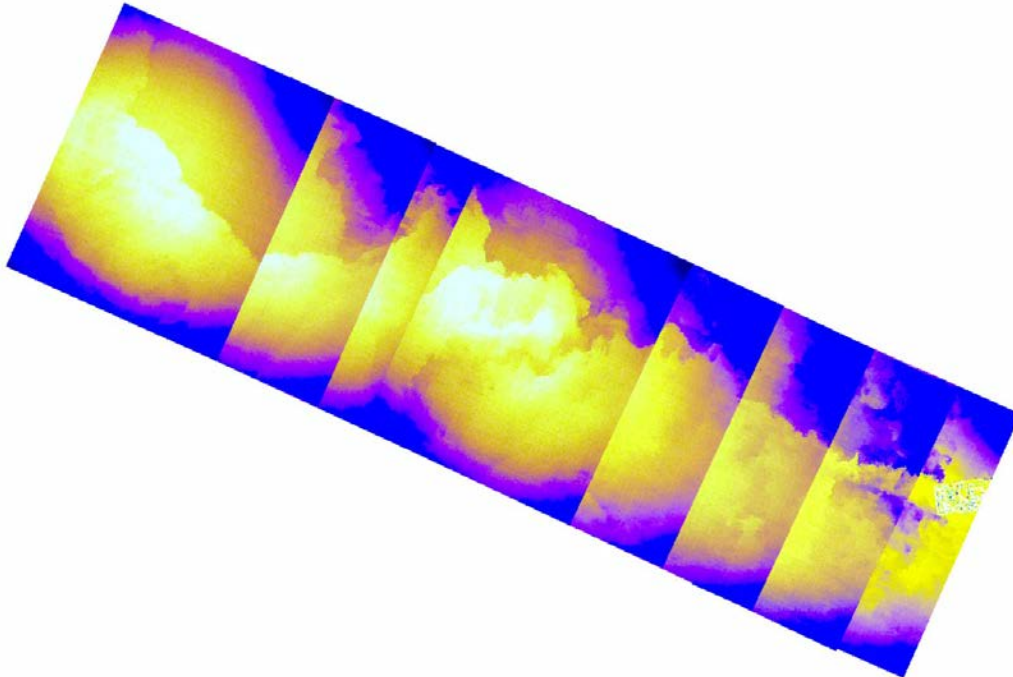


Figure 11. Santa Barbara flight on 08/27/2019 mosaicked and projected with WM FIGS in less than 5 minutes

We performed re-projection of datasets previously collected over spill sites and we were able to georectify imagery that was collected without GPS EXIF information. The example above shows a Santa Barbara flight on 08/27/2019. This short transect is mosaicked and projected with WM FIGS in less than 5 minutes.

2.7 Custom rendering defaults

Four histogram stretching types are available within the ArcMap toolbox. These include:

- **Minimum-Maximum:** Applies a linear stretch based on the minimum-maximum pixel values.
- **Percent Clip:** Removes extreme values by applying a linear stretch to values falling outside the upper or lower bounds, which are defined by the user.
- **Histogram Equalize:** Increases overall image contrast by spreading values within the histogram.
- **Standard Deviations:** Removes extreme values by applying a linear stretch to the values falling within a given standard deviation (n), which is defined by the user.

Each of the stretching types above can be implemented with Gamma Stretching, which enhances the contrast of mid-colors.

Each of these will provide different characteristics for raster layers, and may be appropriate in diverse scenarios. Because the fast export within the FIGS toolbar will take a snapshot of the data frame, the resulting mosaic will be affected by the display properties of the images. Table 3 lists which custom rendering defaults may be best for a given scenario, however, this will heavily depend on the imaging conditions.

Table 4. Example Scenarios for different kinds of stretching

Situation	Potential Stretch for Best Display
RGB Survey with partial Sun Glint	<ul style="list-style-type: none"> • Standard Deviations with Low N and Gamma Stretching • Percent Clip with ~10% Minimum/Maximum
Multispectral Imagery with Land/Ocean	<ul style="list-style-type: none"> • Histogram Equalize • Minimum-Maximum
Thermal Imagery (general)	<ul style="list-style-type: none"> • Histogram Equalize

3 Oil Classification

3.1 Supervised Classification

Supervised Classification methods (such as Maximum Likelihood), require the use of the Training Sample Manager to select Classification Training Samples. The Training Sample Manager is shown below. After the training samples are selected, the “Create Signature File” button can be used to create a “.gsg” file. This is then input to the classification, which is performed by the WM Oil Thickness Classification Toolbar.

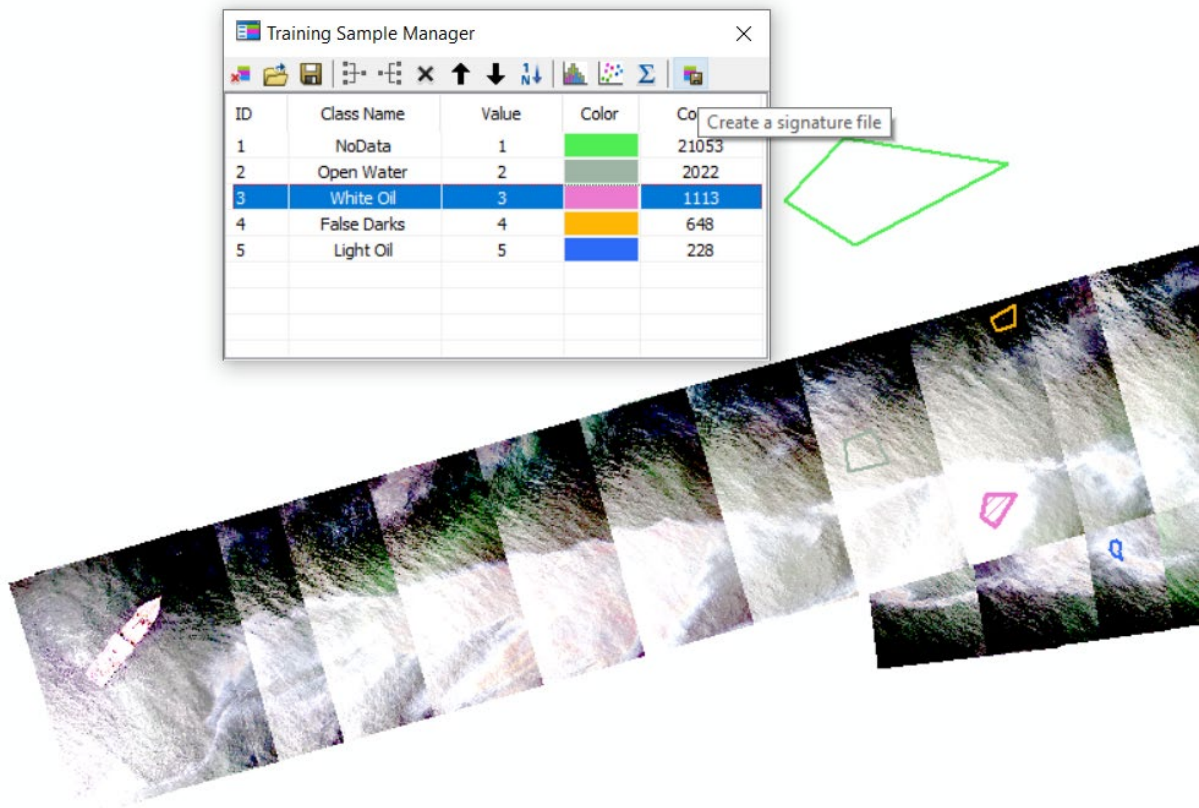


Figure 12. Classification Training Samples

3.2 Example of Raster Classifications

Raster Classifications from Santa Barbara (Flights on 08/28/2019 and 08/29/2019). Fast Export and classifications shown below.

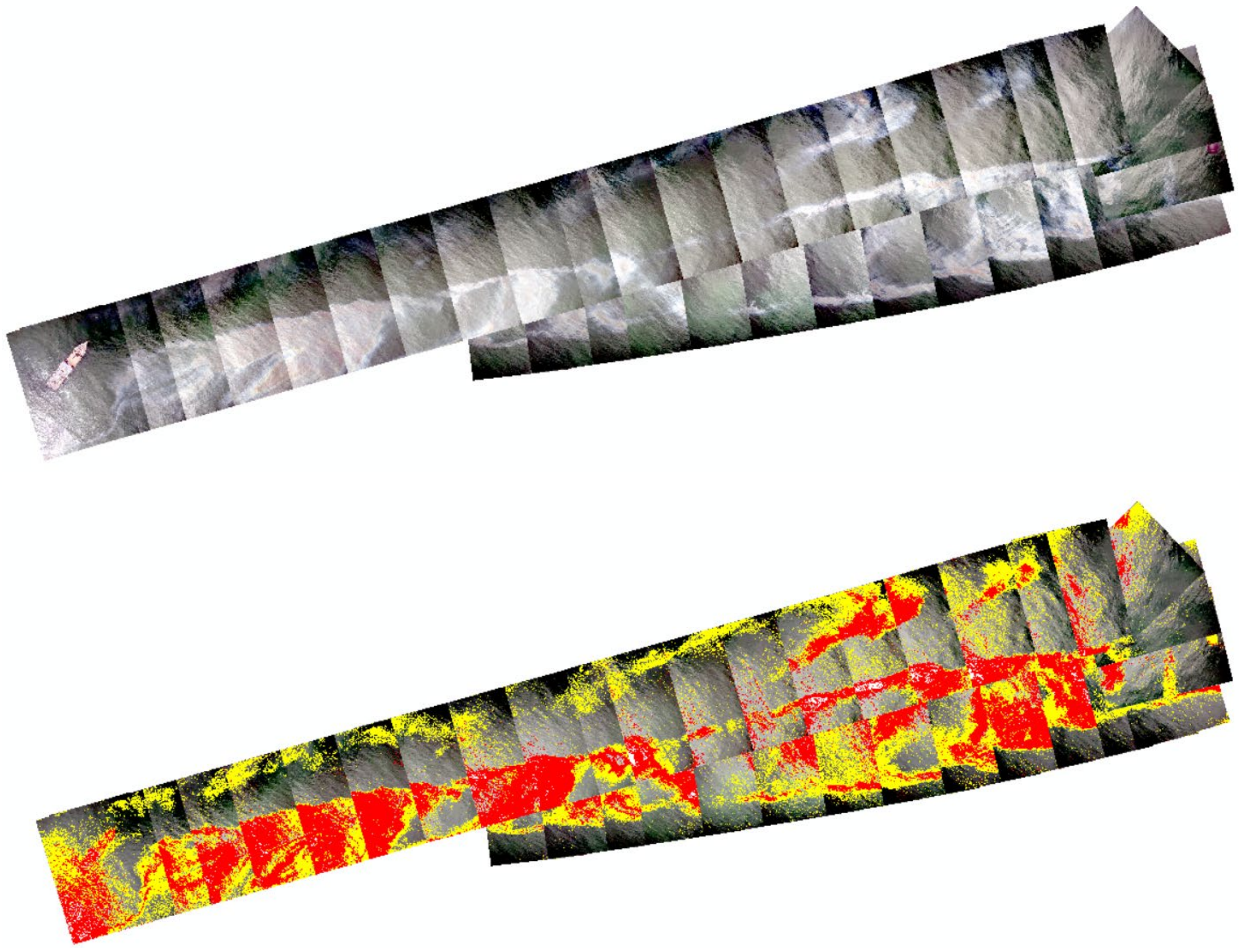


Figure 13. Oil thickness classification

The orthorectification, projection, oil thickness classification of this example above was achieved in 12 minutes. This processing time includes the generation of shapefiles and rasters that can be exported easily in multiple data formats.

4 Technical Documentation

WM UAS FIGS relies on a variety of geocomputational processes to perform the georectification, mosaicking, and classification of imagery. These are specified in this technical documentation in ample detail. The WM UAS FIGS process is described in detail, as well as several different considerations that users and stakeholders should take into account when processing and analyzing derivative products.

4.1 Reading of File Structure

The first step in the processing of a survey's imagery is to define the input directory. After defining the input directory through the pop-up file explorer window, a series of steps is taken automatically by the FIGS GUI. The selected directory is recursively searched for all imagery contained within itself and all child directories. Any image file having ".jpg" and ".tif" extension is recorded on a list. This list contains the filename, the time the snapshot was taken, and the EXIF geotagging information. Snapshots for which EXIF geotags do not exist are then removed from this listing. EXIF geotagged information is assumed to be have a negative longitude (W) and a positive latitude (N). This list of snapshots is then exported to a KML file which is saved in the input directory, with the positions for the image centers as well as filename for each image being recorded. A plot is then generated for all the image locations and shown within the GUI. This plot has a custom update function to allow for the definition of custom labels on the plot tooltips. Plot tooltips are shown and hidden by clicking on each data point. The custom labels contain the Latitude ("Lat:"), the Longitude ("Long:") and the filename ("Name"). The custom labels are calculated by replacing each underscore ("_") with a double underscore ("__") in the filenames, since MATLAB's string parser shows any text following a single underscore as a subscript. Within the custom update function, if multiple images share identical geographical coordinates (and thus are shown by the same point), the first two image names are listed in the custom tooltip. It is recommended that imagery being processed is sequentially numbered for best implementation within the georectification workflow, and that the prefixes to the sequential numbering are strictly non-numerical.

4.2 Defining an output directory

It is generally recommended to define an output directory for appropriate functionality of the various save functions, however, FIGS will run without the definition of an output directory. This has been observed to cause issues with the exporting of the timeline in excel format, and also be the source for general instability during georectification. In cases in which no output directory is selected, the root directory (“C:\”) is used as the output directory. In any case, a folder is created in the output directory at the moment the “Georectify Images” button is pressed. This folder is renamed after a datetime string, and all subsequent processing results are saved in that folder. After the georectification process is completed, this directory should automatically open in the file explorer.

4.3 Selecting the appropriate sensor for the resolution factor

The calculation of a resolution factor for the image georectification process is not a trivial matter. This factor scales both the pixel size and the rotation angle for the image rotation, and has been observed to follow very nonlinear patterns which can be challenging to characterize and vary across different sensors. The resolution factor will also be affected by various flight conditions, such as nominal elevation above ground, and rotation. Table 1 shows the various resolution factors for diverse sensors. Extensive manual testing was performed to calculate the optimal resolution factor for each sensor. Generally, resolution factors are directly correlated with pixel size and inversely correlated to image resolution; that is, a smaller resolution factor will correspond to a smaller pixel size and a higher image resolution. For more information on the impacts between the resolution factor and the georectification of an image, see Section 5.5.

4.4 Defining Survey Lists

In some cases, operators may not wish for all images in the input directory to be georectified. In such cases, operators can use the survey numbers option to only process certain sequences of images. The custom tooltips on the flightplot of the GUI can be used to obtain the name of the images relative to their location on the flightpath. Operators should define a starting and ending image to the sequence they wish to process, and input the numerical portion of their filenames (known as the Sequence ID) into the “Survey List” textbox

separated by a dash (EG: “XXXX-XXXX”). Multiple surveys can be defined separated by commas (EG: “XXXX-XXXX,YYYY-YYYY”). This functionality is also used for flipped flightlines (cases in which the drone was flying opposite to nadir and thus the images are flipped 180°) by adding the letter R after the survey which should be flipped (EG: “XXXX-XXXXR,YYYY-YYYY”).

The strings input into the textbox are split up by commas and dashes to obtain the sequence ID of the snapshots bounding the image sequence. These are then converted to integers, and an inclusive list of integers between the two bounding sequence IDs is then generated. Since the last snapshot in the sequence requires its orientation to be defined (see Section 5.6), the ending Sequence ID is increased by one when possible. The filenames of each of the snapshots in the input directory are then searched for matches to that list; snapshots which match are flagged for inclusion in the calculation. Because the sequence of images is defined according to a series of string matches to the filenames of the images, it is important to ensure that all the images input to WM UAS FIGS have nonnumerical prefixes and postfixes to their sequence IDs to prevent false matches.

Cases in which no survey list is input are treated as a single survey list, with the beginning Sequence ID being defined as the smallest ID found in the input files and the ending Sequence ID being the largest ID found. Since certain sensors number their sequential snapshots according to the radiometric band, a separate survey-list is always generated for each radiometric band found within the input folder. In any case, these lists are used to define the order of snapshots, and thus where each image should be oriented.

4.5 Theoretical basis for Georectification

To illustrate how resolution factors affect the georectification of an image, it is important to review the background of how the coordinates for each pixel in an image are calculated. The following expressions define this relationship: $x = A\hat{x} + B\hat{y} + C$, $y = D\hat{x} + E\hat{y} + F$, where C and F are the x and y coordinates (respectively) of the top-left pixel in an image, \hat{x} and \hat{y} are the column and row numbers (respectively) of the target pixel with respect to the raster's origin, B and F refer to the rotation of the raster, and A and E are the pixel size in the x and y directions for a given image. These expressions will allow to translate from a given pixel location to a projected coordinate (and vice versa) with respect to any coordinate

reference system. For the purposes of this toolbar, images are georectified to the WGS 1984 Web Mercator projection (EPSG: 3857).

To geocode images appropriately, World Files are used. World files contain six lines describing the rotation, positioning, and resolution of rasters. Specifically, factors A – F in the expressions in the previous paragraph are listed in the world files to properly display imagery. It should be noted that world files generally do not contain information on the coordinate reference system. To mitigate this shortcoming, the active data frame's reference system is continually updated to the appropriate Web Mercator (EPSG: 3857) projection.

4.6 Use of EXIF Geotagging for Georectification

The purpose of WM UAS FIGS is to obtain actionable information from UAS surveys for oil spill response operations without the need for lengthy data-driven geoprocessing. Conventional georeferencing (also known as registration) techniques from airborne surveys generally require the acquisition and use of Ground Control Points (GCPs). These high-resolution positional targets can be used within a survey to properly reference the survey to its appropriate location. Regretfully, in the operational environments of oil spills, it is both technologically and logistically challenging to obtain such GCPs. As such, alternative information must be used to georeference imagery; such information can include the geotagging of each image.

Certain imaging sensors record geotagging information within the EXIF metadata of image files. The positional accuracy of such geotags will depend on the accuracy of the onboard GPS receiver for either the UAS or the sensor, depending on the operational scenario, however, this information can be invaluable to appropriately place an within a coordinate reference system. There are several challenges to overcome, however, when using geotags to georeferenced an image. While geotagging information may provide with the approximate coordinates of the image's center, it does not inherently contain information about the orientation of the image. Moreover, although some sensors include altitude within their geotagging information, these measurements have been frequently observed to be inaccurate, and as such, they generally cannot be used to estimate pixel size from manufacturer specifications. Moreover, as discussed in section 5.5, georeferencing of rasters within most

geospatial software is based on the top-left pixel's coordinate, which is not trivial to obtain from the center coordinates without accurate altitude and orientation information. Several steps, as described within this section, were taken to mitigate these challenges.

To mitigate the lack of orientation information, certain flight behavior procedures were adopted by WM survey operators. Specifically, each of the imaging sensors was placed at a vertical (downward-firing) angle aligned with the navigation direction (nadir) of the UAS. In cases with dynamic (remote controlled) gimbals, these were not moved inflight. Inflight, UAS movement was always either nadir or inverse nadir (that is, no lateral movement was allowed). This the use of sequential images to obtain the approximate orientation of each given snapshot. Specifically, since the camera orientation with respect to the drone is not changed between snapshots, and the center of each image is approximately aligned with the UAS, each image can be oriented towards the following snapshot. This approach generally works well for straight flight, but tends to overestimate the rotation of an image during turns. Additionally, since each snapshot is oriented towards the following snapshot in the image sequence, the last snapshot of the survey is not georectified.

To address the challenges in pixel size adjustment, the resolution factor (Section 5.3) was calculated from manual sensor testing. As previously discussed, World Files can be defined based on A, B, C, D, E and F from the expressions $x = A\hat{x} + B\hat{y} + C, y = D\hat{x} + E\hat{y} + F$ (a detailed description of these expressions is provided in Section 5.5). Specifically, each factor is calculated as defined by the expressions below:

$$\begin{aligned}
 A &= RF * \cos \varphi \\
 B &= D = -RF * \sin \varphi \\
 E &= -RF * \cos \varphi \\
 C &= x_{center} - \frac{\cos \varphi n_{cols}}{2} - \frac{\sin \varphi n_{rows}}{2} \\
 F &= y_{center} + \frac{\sin \varphi n_{cols}}{2} + \frac{\cos \varphi n_{rows}}{2}
 \end{aligned}$$

Where RF is the resolution factor, φ is the image orientation, n_{cols} is the number of columns in the image, n_{rows} is the number of rows in the image, x_{center} is the longitude coordinate at the center, and y_{center} is the latitude coordinate at the center. Note that the signs of each of the terms of each equation varies according to φ . As can be surmised from the expressions above, RF varies based the planar units of each coordinate reference system; in this case, the WGS 1984 Web Mercator is used, and as such, all RFs are for meter-centric coordinate systems (such as UTM). Although any other meter-based coordinate system would not see incorrect RF rotations, the origin of each raster would be located erroneously.

4.7 Pressing the Georectify images button

Several tasks automatically take place after the georectify images button is pressed. Firstly, the input directories are checked for a CSV-based flightlog from the UAS. If one is found, it is used to georeferenced images based on timestamps rather than the embedded EXIF geotags. Then, subdirectories within the output directory are created. These colloquially refer to the radiometric bands being georectified, and are used to separate all the saved images accordingly. The filenames of each image are used to classify images. For example, in the M600 sensor, DJI_0001_R would denote a thermal image while DJI_0001 is a visual image. These create a file structure which is later read by the ArcMap ESRIADDIN Toolbar. The processing pipelines vary according to whether a flightlog was found, and are specified in sections 5.8 and 5.9.

4.8 Georectification based on UAS flightlog

The georectification of imagery based on UAS flightlogs requires the installation of a separate version of the MATLAB-based GUI, and is only compatible with the DJI M600 UAS and sensor because of specific formatting of the flightlog. The results from this method may not be compatible with other processes associated with FIGS (such as mosaicking, surveyline identification, etc) since they are georectified using unprojected Coordinate Reference Systems. This GUI includes two additional textboxes for a time offset and a reference time to ensure time synchronization between the UAS, flightsensors, and UTC. When this version of the GUI is installed, and a flightlog is found, column headers are scanned to ascertain which data is

included in the flightlog. The following strings are searched, based on common strings generated by flightlog translation software:

- “datetime(utc)”
- “gimbal_heading(degrees)”
- “gimbal_pitch(degrees)”
- “altitude(feet)”
- “time(millisecond)”

Considering that there may be certain time offsets between the timing devices onboard the UAS and UTC, a time offset field must be calculated to correct these disparities. A reference UTC time is collected by imaging a tablet displaying UTC at the beginning of a flight. This reference image filename is then input on the first textbox, and the time displayed on the tablet is input to the second textbox. The EXIF tags in the reference image are scanned for a time, and that time is subtracted from the time input in the second textbox. This time offset is then applied to the flightlog within the UAS to properly georectify imagery. After the time offset has been applied, the gimbal angle, and geolocations for each image is interpolated from the flightlog. These are then used to calculate the parameters within the world file for each image as specified in Section 5.6. Each image is then copied to its respective output folder (which is identified according to the radiometric band), and the world file is written to that same folder. After this process is completed, a file explorer window is launched at the output directory, which indicates this process has succeeded.

4.9 Georectification without a UAS flightlog

Once the images in the surveylines have been identified, their geotagging information is assimilated and converted to decimal degrees. The images in rotated flight tracks are then flagged for rotation. Within MATLAB, a python installation under the root directory (“C:\Python37_64\python.exe”) is loaded and then used to convert these geotags to Web Mercator. This is performed using a python library named pyproj [cite]. The rotations of the images are then calculated, and the world file is generated (Section 5.5). The surveylists (which can be either user-defined or program-defined as described in Section 5.4) are used to define the image sequence, with the general pattern being that images with higher image IDs (as identified in each filename) are assumed to be taken after lower image IDs. When no UAS

attitude information is available to define the rotation angle, images are rotated towards the center of the next image in the input file. The output filename is derived from the raster's input filename, with a prefix added to indicate the surveyline each image belongs to. This export is an iterative process, which concludes once all the images in the survey list have been processed, copied into their respective output folders (as identified by the radiometric band), and had the world file written. After this process is completed, a file explorer window is launched at the output directory.

4.10 Translating EXIF Geotags to images without EXIF tags

EXIF geotags are usually embedded onto images by the sensor, however, some sensors do not have the required GPS receiver or do not embed the imagery for alternative reasons. In such cases, and when another sensor on the same survey collected images with EXIF tags, images can still be georectified in FIGS. To do this, a timeseries is generated translating the EXIF geotags from the geotagged images and saved to a spreadsheet. Then, a shell command is used to add geotags based on a timeseries through a third-party tool, EXIFTOOL. These images can then be put through the regular processing pipeline.

4.11 Reading the georectified imagery into the ArcMap Document (.mxd)

ArcMap is capable of drawing rasters without embedded georectification tags (also known as GeoTIFF tags) through the use of a world file, which is described in Section 5.5. World files generally do not contain information about the coordinate reference system to which they are referenced, as such, when importing images with world file geotagging, it is important to ensure that the map documents' projection matches that of the world file. Users are able to manually import the georectified rasters (which are exported as discussed in Sections 5.8 and 5.9), however, WM FIGS also provides an automated import option. To make use of it, users should save their map document in the output directory. This directory was chosen by the user at the beginning of the georectification process, and is launched in a file explorer window after all the images are georectified. After the map document has been saved, users can select the option "Read files" in the WM ArcMap georectification toolbar. This procedure is detailed in this section.

To import a raster programmatically, ArcMap requires the creation of a custom layer file (.lyr), which contains metadata on the image file, its georectification, and display parameters. This file is created automatically through the use of the Python 2.7 extension ArcPy, and saved to the same directory as each raster with the same name. After the layer file is created, the rasters are successively imported into ArcMap. It should be noted that this process can become protracted when importing a large number of images. For this reason, a prefiltering step is recommended for all imagery obtained from the UAS (as discussed in Section 5.15). Rasters are imported into separate group layers according to their radiometric bands and surveylines, as indicated by their exported filenames.

4.12 Mosaicking

Exporting all the georectified rasters as a single still generally simplifies analysis, as such, WM FIGS provides several options to this end. These are “Fast Export” and “Quality Export”. Fast export relies on the copying of the ArcMap canvas, while the quality export relies on the ArcPy “Mosaick to new raster” tool. As their namesakes imply, the Fast Export will be much swifter than the quality export, at a penalty in resolution and color fidelity. Each of this processes is explained in more detail in this section. After the mosaics are exported, their NoData value is set to the background color of the canvas (white). This signifies a 255 value for 1-band rasters and a (255,255,255) value for 3-band rasters.

The fast export option draws the ArcMap canvas into a GeoTIFF. This is performed through the ArcPy “ExportToTIFF” instruction. The resolution combobox option defines the amount of pixels in the longest dimension of the output raster. For example, the default option, 3000, will result in a GeoTIFF of 3000 pixels on its longest side. From this pattern, it is apparent that larger surveys will see a starker decrease in resolution from using the Fast Export, however, this also signifies that export times will be very similar regardless of the actual survey size. Each Group Layer in the active dataframe of the map document is exported separately to ensure that different flightlines and radiometric bands have separate rasters, and all of the exported mosaics are automatically imported into ArcMap. Although this process also calls for the automatic conversion of the exported GeoTIFFs into a KMZ file, this has been observed to frequently fail or produce corrupted files due to issues with the ArcPy conversion mechanism.

The quality export option merely a shell operation to the ArcPy Mosaic to New Raster tool, which is applied for each group layer in the active data frame of the map document. All of the visible images are included in the exported mosaics, and these are added to the map document and automatically exported to a KMZ file. While exporting the desired mosaics, users may encounter certain snapshots which they do not desire to include in the mosaic. Users are able to simply turn the visibility of these layers off, or alternatively, remove them from the map document entirely. Either of these will ensure that neither the Fast Export nor the Quality export includes the undesired snapshots in the exported mosaics. To reduce stitching errors and misalignments, users may also opt to only include every second or every third snapshot collected by the UAS. The Skip Combo box will automatically turn n consecutive layers off, starting with the first layer of each group layer. As explained, this will automatically exclude these layers from any exported mosaics.

4.13 Training Samples

Training samples are used to identify the characteristics of the desired output classes for supervised classification algorithms. Because unsupervised classifiers have been observed to underperform supervised classification in oil spill monitoring, the collection of training samples is necessary for the creation of appropriate actionable products from a UAS survey. Ideally, training samples should only contain the most exemplary pixels for a given class to maximize the performance of the classifier, while also providing appropriate representation for the entire survey. As such, it is recommended that training samples are collected throughout the entirety of a survey's extent to encompass all of the imaging conditions in the mosaics. Moreover, it is recommended that multiple classes for background (non-oil) pixels be created, to ensure that oil extents are best classified. These may include separate classes for any land, vessels, water bodies, or marshes present in the survey.

To collect training samples, the Training Sample manager allows users within ArcMap to draw polygons encompassing the desired region of interest. These can then be labeled with a string, and assigned a value for the classification. Training samples can be merged (this process simply assigns two training samples the same value within the output signature file) and deleted. Moreover, training samples can be saved as a polygon file for future reference and to

examine the performance of the classifier ex-situ. It should be noted that a signature file does not contain the selected training samples, simply their summary statistics to provide to the classifier.

In certain cases, the separability of the classes can be analyzed through the histogram and scatterplot options in the Training Sample Manager, however, this functionality has been observed only to function when input rasters have an 8-bit color depth, and the functionality heavily depends on the ArcMap installation and the system at hand. Although the amount of pixels in a training sample for a class has not been observed to directly impact the performance of the classification, it is generally recommended to keep a balanced amount of pixels across all the training samples to ensure that outlier pixels are not inadvertently introduced into the classification.

4.14 Classification

WM FIGS relies on supervised classification to provide with rapid oil extent maps. To this end, training samples are collected using the ArcMap Training Sample Manager, which contains several options to create, merge, and export training samples, as previously described. Training samples are statistically summarized in a signature file (.gsg), which is then input into the supervised classifier to provide with accurate delineations of the input classes. Once the Training Samples have been collected, the “Classify Oil” tool within WM FIGS will accept the signature file as an input, along with the mosaicked raster, a polygon mask (which indicates which portions of the raster should be included in the classification), and the output directories for the classified raster and polygon shapefile.

The Classify Oil tool performs several geospatial processes successively, which are detailed in this paragraph. First, the input raster is masked with the mask layer to ensure that areas outside the desired processing region are not included in the classification process. Then, this masked raster is input into a Maximum Likelihood Classification along with the signature file. This exports a classified raster along with a classification confidence raster, which contain a number of classes equal to those defined in the input signature file. The classification confidence raster is an optional output of the Classify Oil tool. The classified raster stemming from the supervised classification is then input to a vectorization (IE, Raster to Polygon)

method. Since this output will likely contain several small polygons due to singular pixels being identified as different classes, the output of the vectorization is dissolved exported as the final polygon layer. These actionable layers can then be provided to stakeholders for the appropriate response to the oil spill event.

4.15 Prefiltering Imagery from the UAS

While WM FIGS automatizes many of the time-consuming tasks related to the generation of actionable products for oil spill response, there are certain scenarios in which some manual pre-filtering of the UAS data can greatly speed up processing time. Specifically, in surveys with a large amount of stationary snapshots, it is useful for these snapshots to be removed from the input folder for WM FIGS. This is since adding a large amount of rasters into ArcMap increases the processing requirements, and as such, makes the georectification, mosaicking, and classification process much longer. Moreover, it is also recommended that all snapshots are renamed so that the sequential identifier (known as an image ID) is the only numerical portion of the filename. This ensures that the image sequence is appropriately identified within the georectification step, and snapshots are oriented appropriately.

Table 5. Resolution Factors for various sensors at 400 ft AGL

Sensor	Resolution Factor at 400 ft AGL
M600 Thermal	0.170
M600 Visual	0.032
Micasense 5-band	0.058
GoPro	0.050
Thermal Non-EXIF	0.250
HT20	0.0462

5 Phase 2: Calibration and testing of sensors.

For the calibration and testing of the sensors for detecting variations on oil thicknesses, we took the opportunity of performing multiple experiments at the United States Army Corps of Engineers Geophysical Research Facility (GRF) of the Cold Regions Research and Engineering Laboratory (CRREL) in Hanover, New Hampshire. CRREL's Geophysical Research Facility's (GRF) outdoor test tank had approximately 10 to 12-inch-thick ice sheet cover at the start of the study. CRREL staff cut out 12 individual squares (1m x 1m) from the ice sheet; they served as individual treatments for synoptic UAS and physical measurements of oil thickness data collections (Figure 14). CRREL staff added broken ice to individual squares to cover a range of percent ice cover (no ice as control, 5-10%, 25%, 50%, 80%). These percent ice cover treatments were used throughout the experiments. Eighteen black plastic totes, each with a unique thickness and or oil type, provided a point of reference for the reflectance of thermal and spectral radiation for calibration for the UAS sensors (Figure 15 and 16). The totes were black to avoid reflections from the bottom or ice.



Figure 14. Ground view of the GRF tank with ice squares (1m x1m) and black plastic totes for oil thickness calibration.


N 	No Oil	10 μm	50 μm	100 μm	200 μm	← Fresh ANS
	No Oil	10 μm	50 μm	100 μm	200 μm	← 50/50 Emulsion
		500 μm	1000 μm	2000 μm	5000 μm	← Fresh ANS
		500 μm	1000 μm	2000 μm	5000 μm	← 50/50 Emulsion

Figure 15. Target thicknesses of each tote for reference of spectral and thermal reflectance. These known amounts were used for calibration of the UAS sensors.

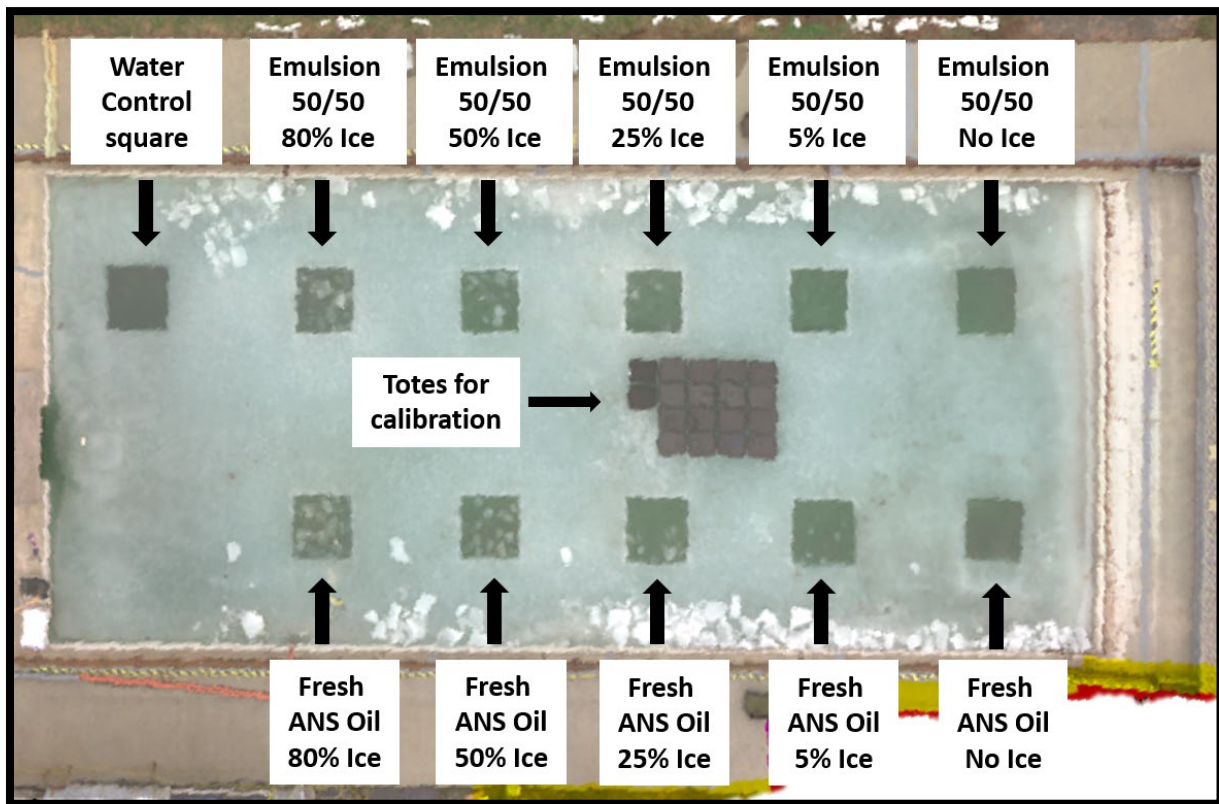


Figure 16. Aerial view of the tank setup before oil was added to the squares.

Each of the maps or aerial photographs shown in this report (e.g., Figure 13) was made by stitching a number of individual still images to create an orthomosaic (i.e., multiple photos collected from different positions as the UAS was flying the tank at low altitude (13.7 m).

More than 5,000 digital multispectral, visual, and thermal photos were taken during the 24 hr time lapse experiment. Thermal imagery was obtained using a Forward Looking Infrared (FLIR) camera that was calibrated for the collection of relative apparent temperature data on each pixel in the image. To process and analyze the time lapse data, an algorithm was generated that batched the images to process them semi-automatically. This algorithm extracted the apparent temperature data from locations and targets selected manually. These targets included areas within the totes where variations in thermal radiance could be visually detected with respect to variability on the oil thickness. Additional targets were selected within the area of the 1 m x 1 m squares to compare different oil thicknesses and emulsifications with ice and water. The apparent temperature values were compiled on data processing software and used for statistical analysis. Figure 17 shows an example of the thermal imagery. The positioning of the A-frame holding the sensors above the totes allowed directly sun exposure and some shading (indirect sunlight). Unfortunately, the alignment of the camera was not perfectly aligned with the totes. This occurred because it was very difficult to position the camera on the A-frame from ladders positioned on the ice sheet.

The totes on the center of the GRF tank, provided another way to measure the variability of the apparent temperature of the oil as a function of oil thickness. Figure 17 shows the visual true color of the totes, the thermal view, and range of apparent temperatures inside each tote during Flight 4 (08:34 am, overcast conditions) . Box 1 (water only, non-emulsified oil) had an average apparent temperature of 48.7°F, while the 10 μm tote (Box 2 non-emulsified oil) had an apparent temperature of 50.8°F. The apparent temperatures of the boxes inside the non-emulsified totes keep increasing until reaching 55.5°F for the box with 5,000 μm of oil (Box 6). These data demonstrated that when there is no ice included on the surface under analysis, the apparent temperature is directly indicative of thickness.

The oil distribution in some of the totes was uneven. This occurred occasionally because of a disturbance to a tote's surface. For example, when the UAV flew closer to the ice surface, the propeller downdraft (prop wash) occasionally caused air currents (downdrafts) across the a tote's surface causing a non-uniform oil distribution (e.g., accumulation in one part of the tote).

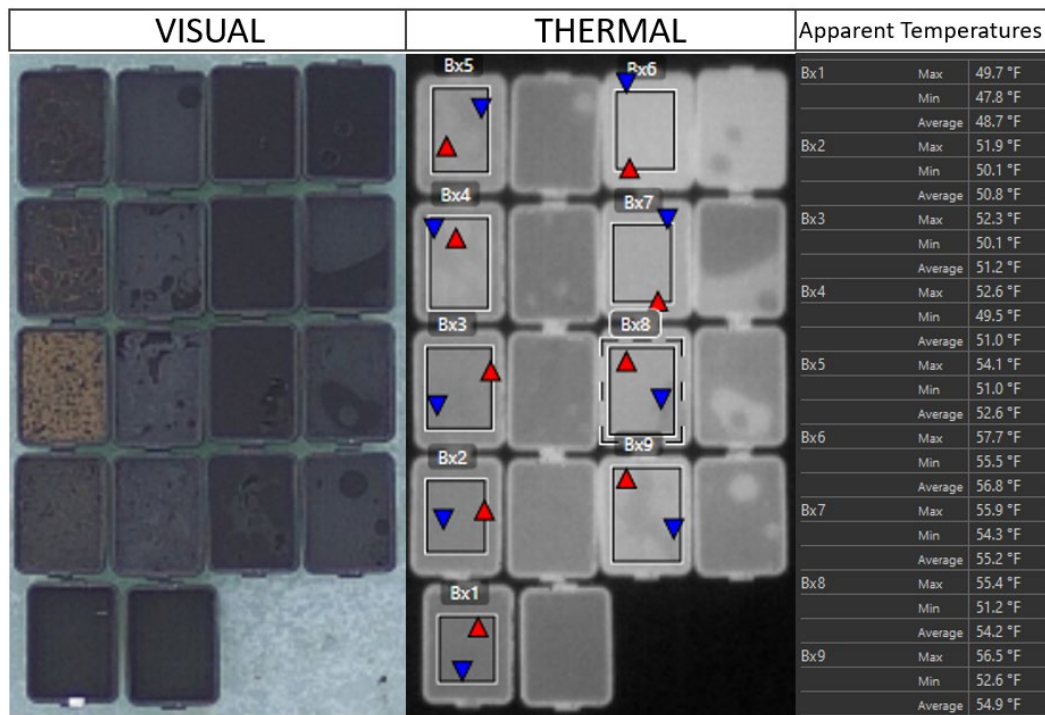


Figure 17. These measurements show the maximum (red triangle), minimum (blue triangle), and average of the apparent temperatures inside the totes (Boxes 1 through 9). Flight 4 at 08:38 hr local time, overcast conditions.

The maximum, minimum, and average apparent temperatures of the totes were compared among flights. During Flight 4, there were two domains. These data were collected at 8:34 am of the morning under overcast sky conditions and limited solar radiation. These low illumination conditions were chosen for analysis because they represented the most challenging scenario because the thermal radiation from the sun was low enough so that the range in apparent temperature readings only $\sim 7^{\circ}\text{F}$. Under cloudy conditions and early in the morning, Figure 18 demonstrates that change in the oil thickness was only easily detected for slicks $\leq 500 \mu\text{m}$. While the thermal radiation of thickness $> 500 \mu\text{m}$ show very little variation (tailing effect). Early in the day (and under dense cloudy conditions), the sun has not warmed the thicker oil layers and they do not have different reflective apparent temperatures. Early in the morning, when there is very little variation in the apparent temperatures, oil thickness classification with low altitude thermal sensors will likely be extremely difficult. This will also apply to any Arctic conditions with low solar radiation on an the oil slick.

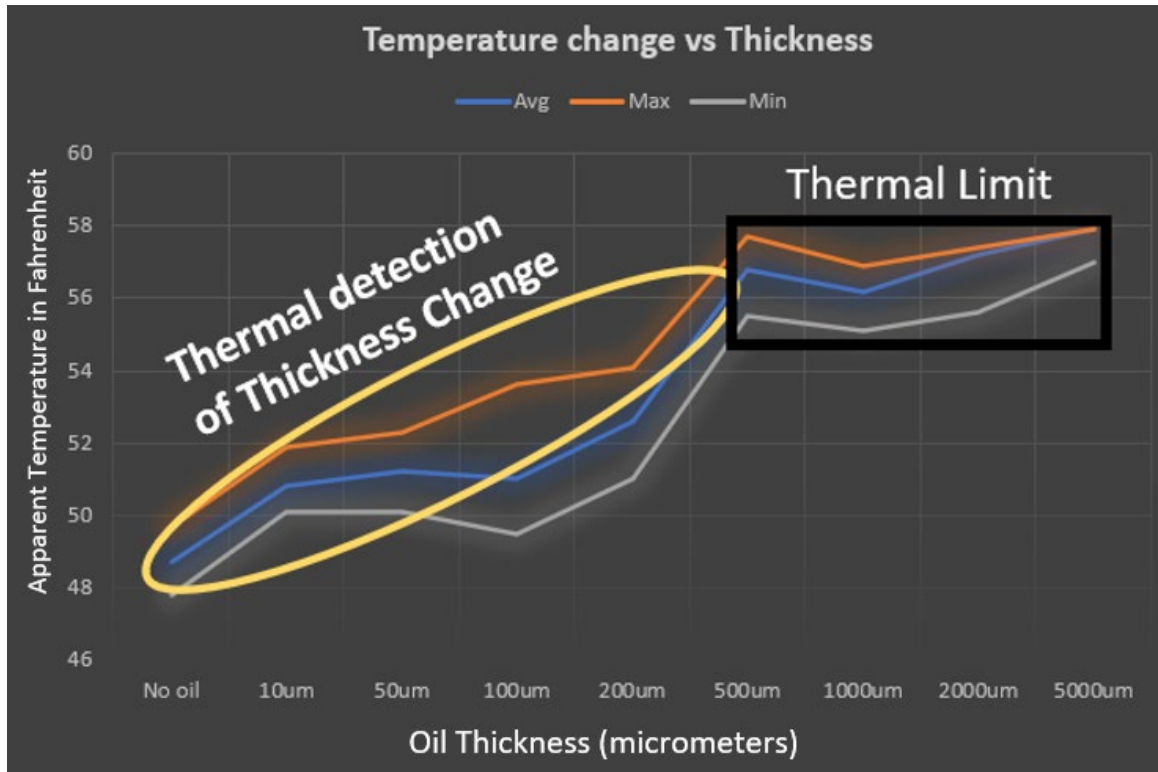


Figure 18. Comparison of maximum, minimum, and average of apparent temperature observations for the totes vs oil thickness during Flight 4 at 8:34 AM under overcast skies and limited solar radiation.

UAS Flight 7 at 11:34 am had more solar radiation. Skies were still overcast, but light from the sun could be seen at least reaching the totes indirectly. Under these conditions, the distinction among oil thickness was more favorable (Figure 20) and the tailing effect above 500 μm was not seen. Instead, the steady increase in apparent temperature was expanded up to the maximum thickness of 5,000 μm . The linear relationship indicated the apparent temperature on the totes increased 1.22 fold starting at 49.9°F as the thickness of the oil increased:

$$A_T = 1.225 O_T + 49.908 \quad (\text{Equation 1})$$

where A_T is the apparent temperature (°F) inside a tote and O_T represents the corresponding oil thickness (μm). This linear relationship only applies for the conditions present at the time these multispectral images were taken. Stronger intense thermal radiation will increase a separation on the apparent temperature values of the thicknesses. Similarly, as seen earlier in the morning

(Figure 19), less thermal radiation will produce less contrast and it may reach an inflection point above which apparent temperature changes little with increasing oil thickness.

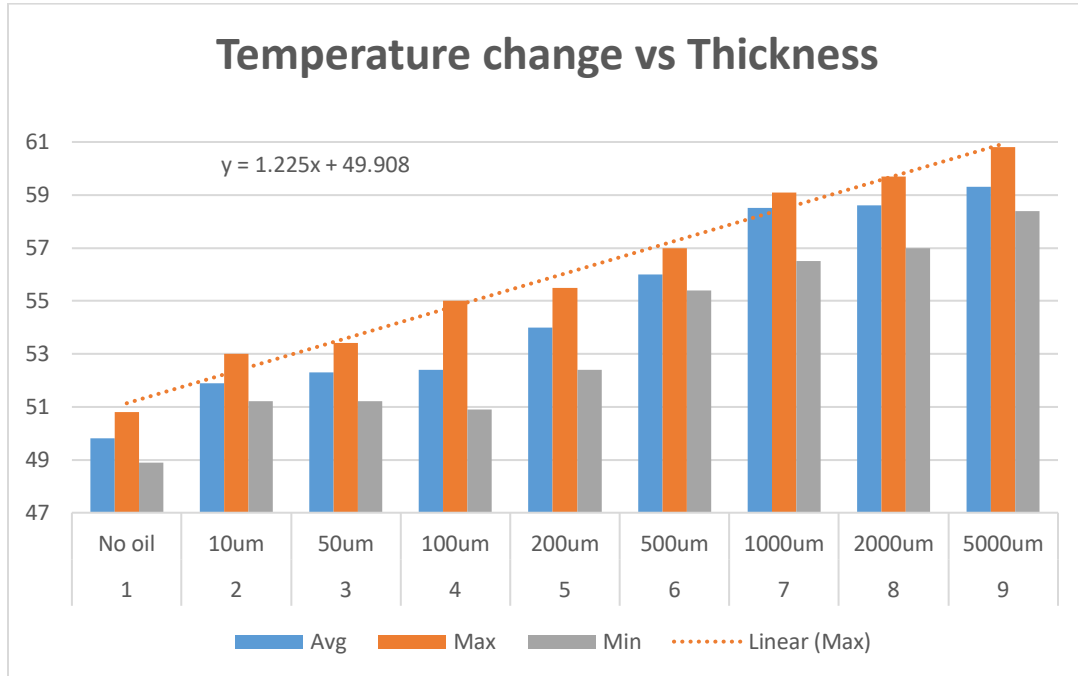


Figure 19. Apparent temperature change vs oil thickness for Flight 7 at 11:34 am under overcast skies, but with more solar radiation.

More than 5,000 digital multispectral, visual, and thermal photos were taken during the 24 hr time lapse experiment. Thermal imagery was obtained using a Forward Looking Infrared (FLIR) camera that was calibrated for the collection of relative apparent temperature data on each pixel in the image. To process and analyze the time lapse data, an algorithm was generated that batched the images to process them semi-automatically. This algorithm extracted the apparent temperature data from locations and targets selected manually. These targets included areas within the totes where variations in thermal radiance could be visually detected with respect to variability on the oil thickness. Additional targets were selected within the area of the 1 m x1 m squares to compare different oil thicknesses and emulsifications with ice and water. The apparent temperature values were compiled on data processing software and used for statistical analysis. Figure 21 shows an example of the thermal imagery.

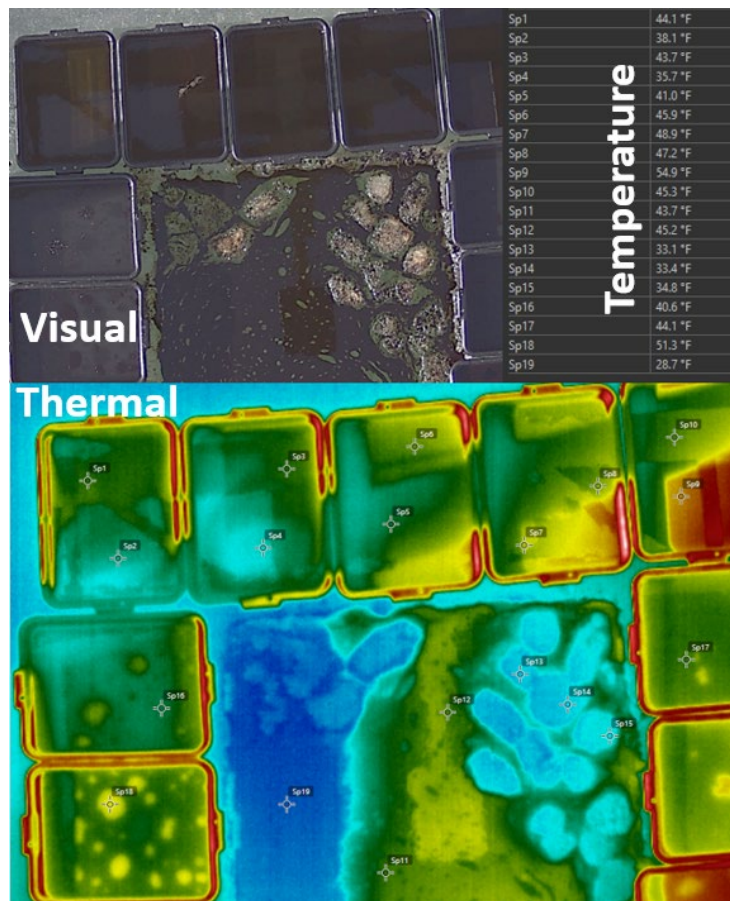


Figure 20. Example of difference in imagery obtained from the visual versus thermal sensors The top photo is a visual RGB image in which little can be discerned much about the variation in thickness as opposed to the apparent temperature data in the bottom image.

Figure 21, a plot of the apparent temperatures for the oil targets inside the totes, showed the emissivity (relative apparent temperature) properties for thicknesses and oil types where the camera was able to capture images. The effect of the sun crossing overhead, setting, darkness, dawn, sunrise and the sun again crossing overhead is clear in the apparent temperature pattern over the 24 hr time lapse from noon to noon.

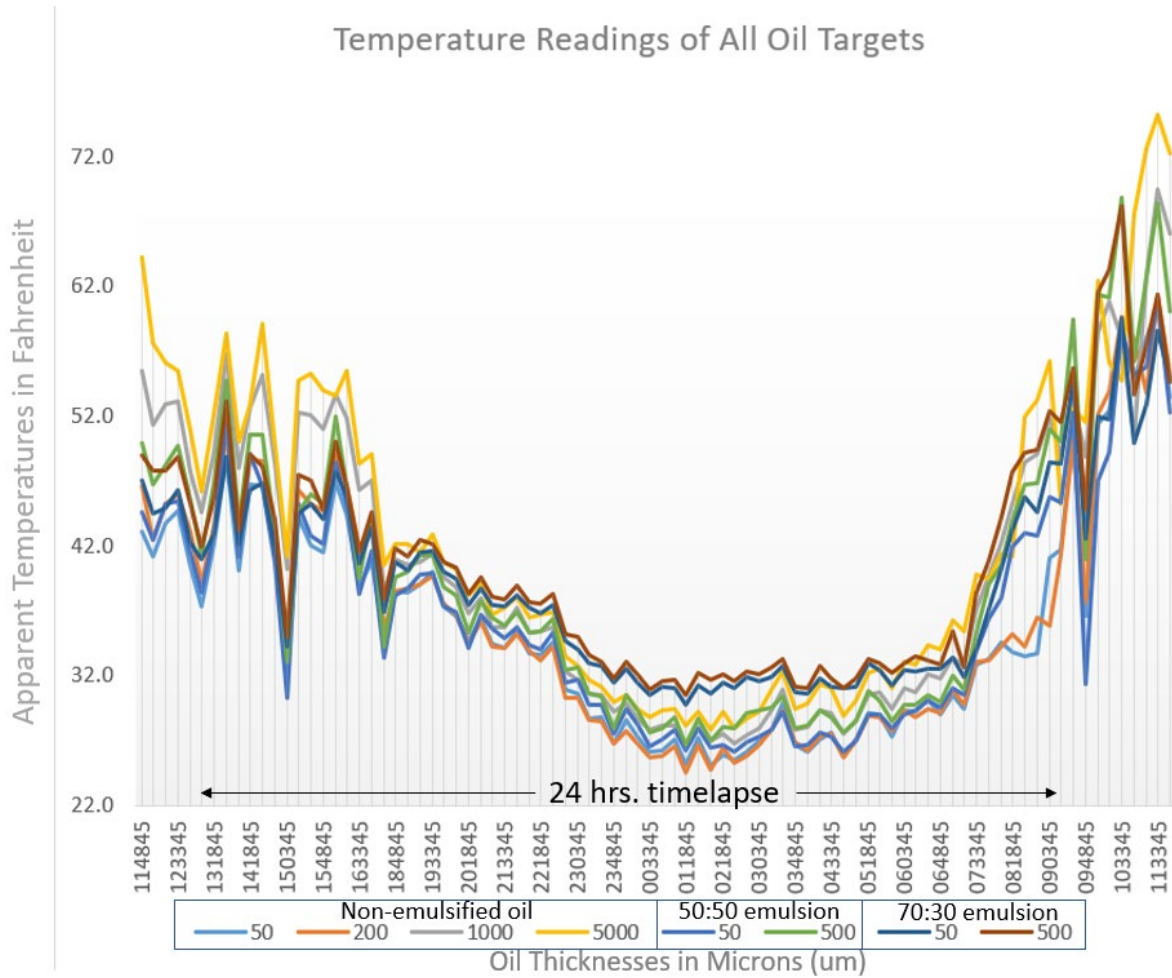


Figure 21. Thermal readings from the 24 hr time lapse of oil thicknesses for the totes. Each point is the average of apparent temperature readings every 15 minutes.

For subsequent discussion, only the non-emulsified data will be shown, but the pattern in the apparent temperatures for the emulsified oil (50:50, 70:30) was similar. Apparent temperature readings from the 24 hr time lapse of non-emulsified oil shows the persistent effect of the thicker oil on the thermal radiation reflectivity under these cold ‘Arctic’ conditions (Figure 21). While the thermal difference between 50 and 200 μm of oil thickness was minimal (maximum difference of 4°Fahrenheit), the difference between 50 and 500 μm, 50 and 1000 μm and 50 and

5000 μm reached 13°F, 18°F, and 25°F, respectively. 50 μm was used as a reference because it is typically the threshold for ‘actionable oil’. This is similar to the quasi-linear relationship observed for the totes during the low altitude thermal analysis (Figure 22).

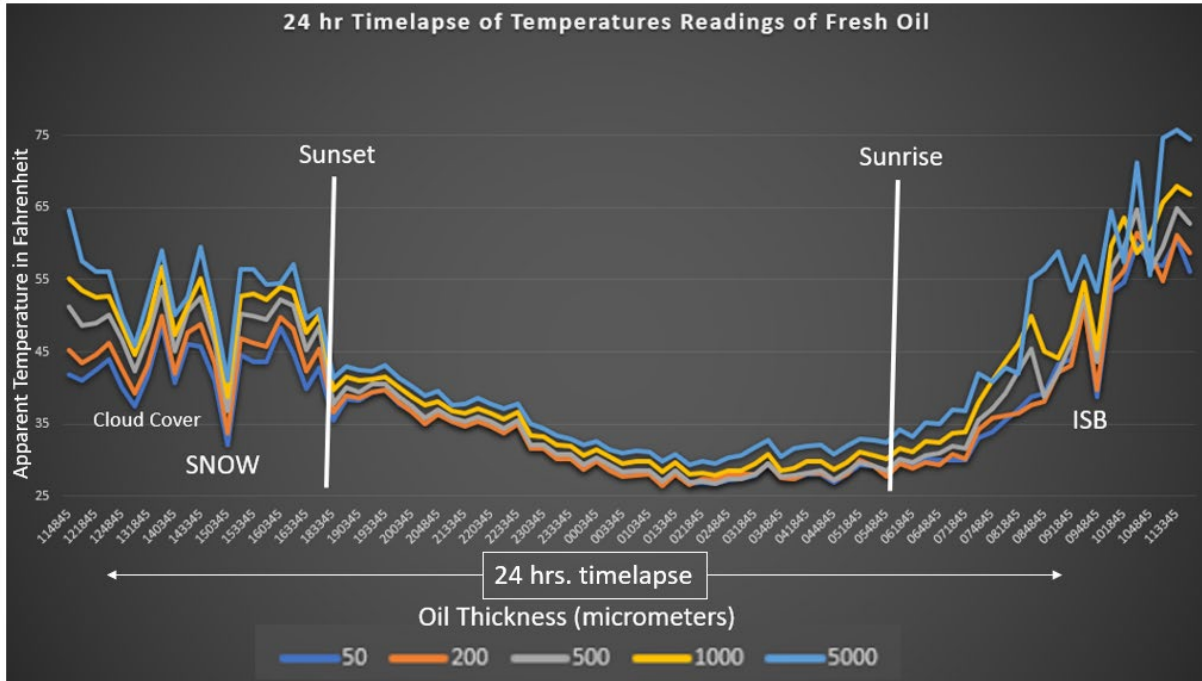


Figure 22. Apparent temperature readings of non-emulsified oil over a 24 hr timelapse

The apparent temperature readings for oil slicks measuring between 50 μm and 200 μm were very similar, indicating that the capacity to discern thicknesses in this range thermally may be limited. There are several reasons for this limitation. For example, thin oil slicks tend to be more susceptible to surface water effects and much more unstable. This leads to general tendency for thinner oil slicks to agglomerate together after some time introducing uncertainty to oil thickness estimates and unexpected oil behavior. Another reason for the lack of thermal discernibility in thin oil slicks is the spectrum of the sensors used, which limited the ability to resolve the differences between them.

It snowed during the evening of the April 22nd. This was captured by the low apparent temperature reading (Figure 22). Before the snow, the project team captured the effect of dense cloudy conditions when solar radiation was drastically reduced. Sunset and sunrise were also

very apparent and during the night there was a tailing off of the signal and a minimal difference in the apparent temperatures for the oil, regardless of thickness. Once sunrise occurred the oil began to warm, slowly at first and then rapidly.

The thermal readings of non-emulsified oil, and 50/50 and 70/30 emulsions were fairly similar for the same thicknesses (Figure 23). The effect of the water molecules in the 70/30 emulsion produced an inversion on the level of radiation as the sunlight disappeared at night indicating that highly emulsified oil may have a greater apparent temperature at when light levels are very low to non-existent in the Arctic.

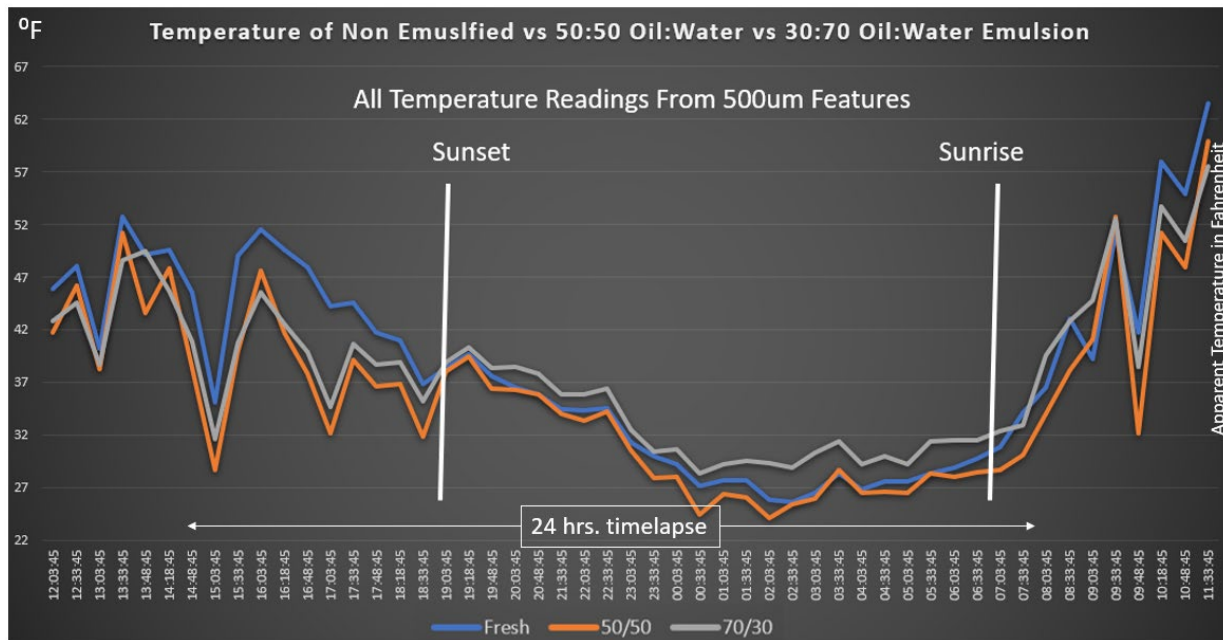


Figure 23. Apparent temperature of Non-Emulsified vs 50:50 Oil: Water vs 30:70 Oil: Water Emulsion

6 Phase 3. Testing of the algorithm in the field.

The first test on the field consisted of verifying that the format of the produced data was compatible with platforms that responders could use. In this case we tested the data formatting for the ERMA platform after we conducted multiple survey missions at the Santa Barbara Seeps. We used archived UAS data and new data to test multiple settings of datasets fully customized to be ingested by the NOAA ERMA system. In this example we can see a full UAS dataset that was processed and delivered in less than 20 minutes.

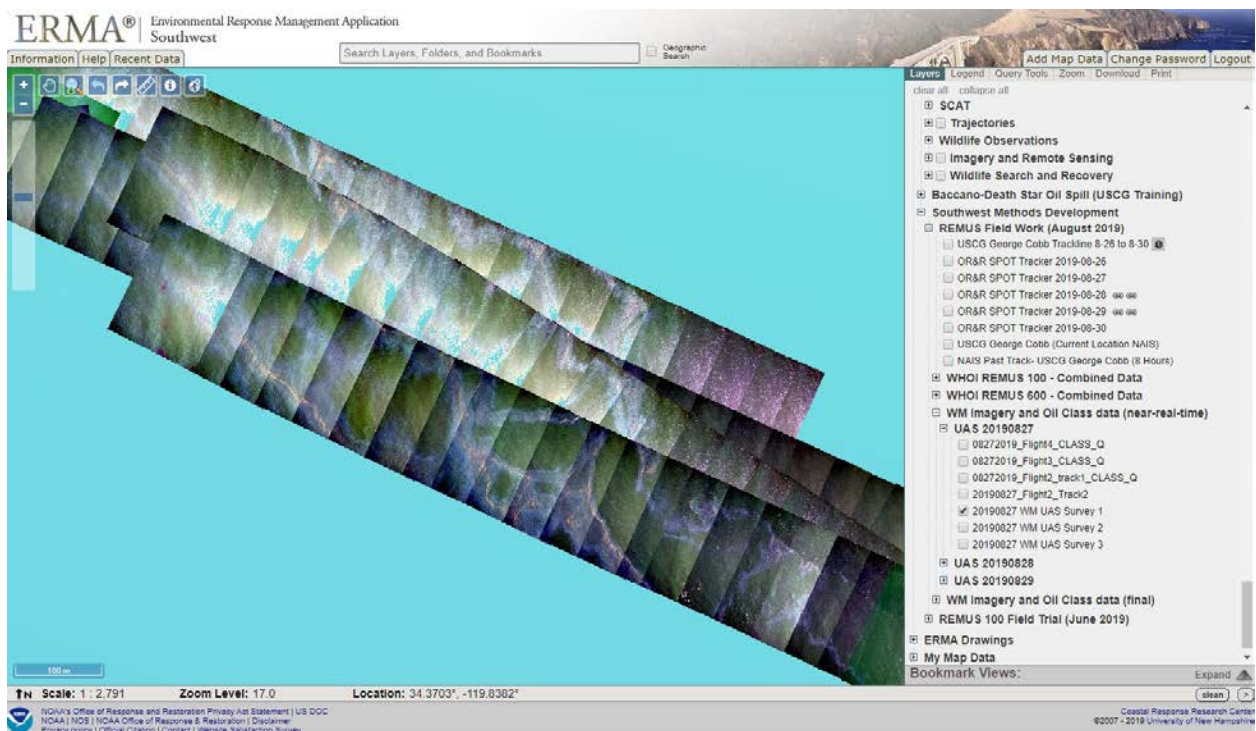


Figure 24. ERMA interface showing a collection of UAS flights that overlapped

These maps now can be made available on the online system on near real time. In this example below we can see with more detail a subsample of the previous map displayed on the ERMA site. During the second week of May of 2021 we conducted a field work campaign over the seep sites in Santa Barbara for testing of the system. The performance of system exceeded our expectations. After confirming that projection of the imagery was very accurate, we could also

verify the scale of features like the size of vessel and the distribution of the oil slick with the thick actionable oil (Figure 25).

6.1 Production of UAS orthomosaics in near real time.

In the example shown below we covered a transect of approximately 1.5 miles long. The flight path shows that the direction of the UAS had to be adjusted so most of the oil could be captured on scene. The projection of the individual stills shows a proper location on the map as they display the sequence of the oil with an outstanding alignment.

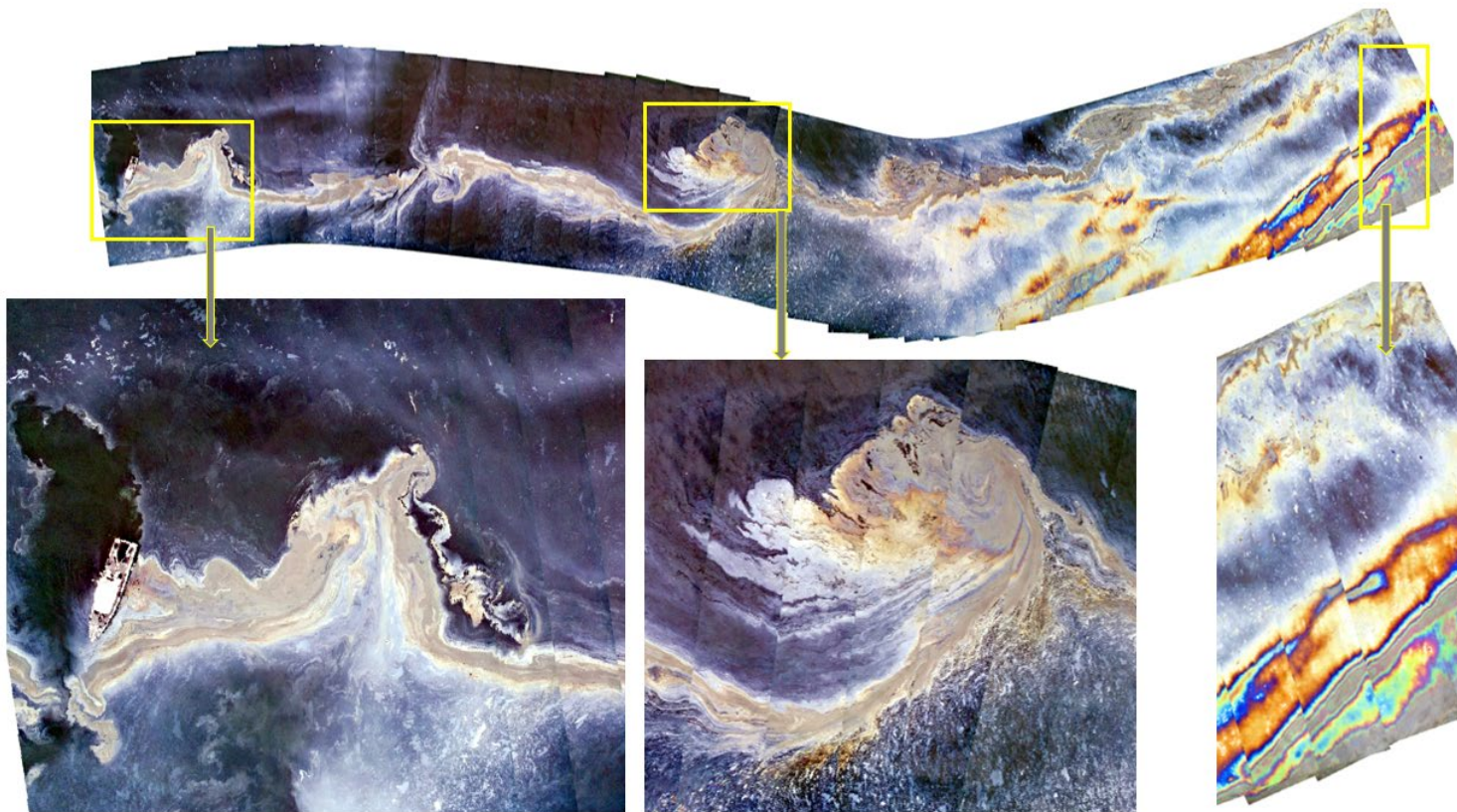


Figure 25. Orthomosaic of the oil slick with detailed zooms to appreciate the level of detail of the imagery.

The field campaign on May of 2021 allowed us to validate our methods for projection of the imagery. This was verified on multiple occasions with surveys flown in different directions. Figure 26 through 29 shows examples of those surveys after being projected.

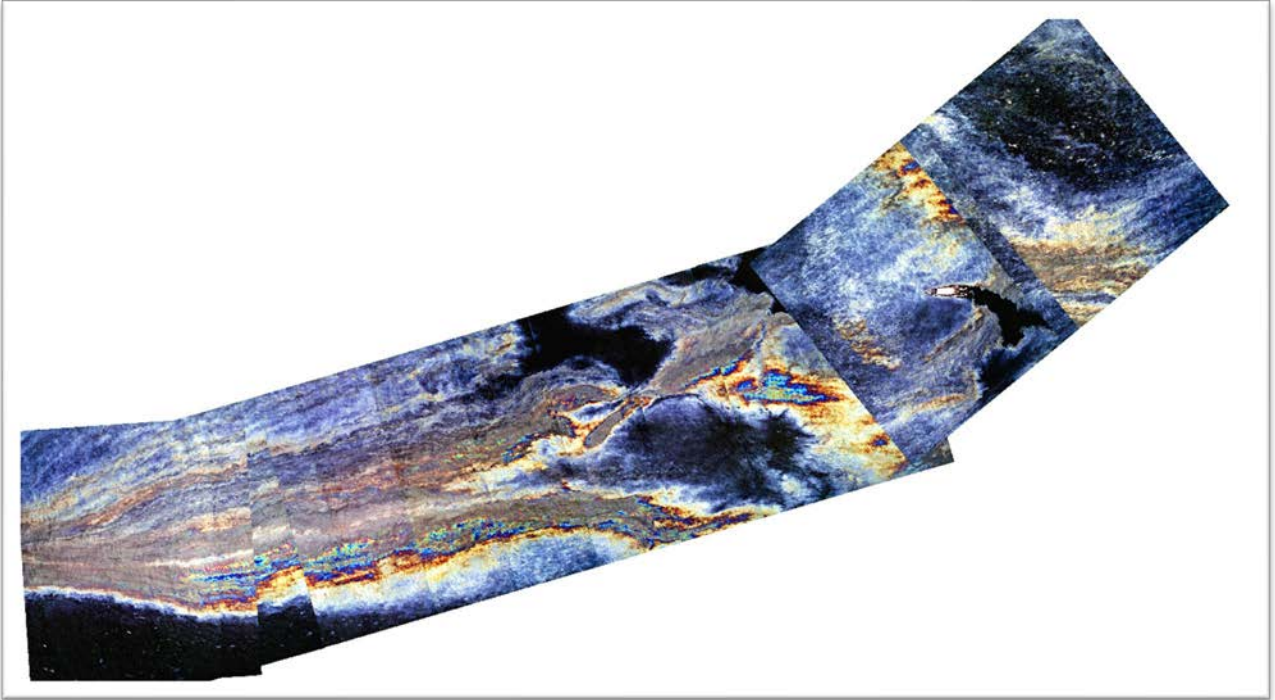


Figure 26. WM_UAS_0511_1216Survey1, collected on May 11 at 12:16PT



Figure 27. WM_UAS_0511_1402Survey2, collected on May 11 at 14:06PT



Figure 28. WM_UAS_0511_1421Survey3, Collected on May 11 at 14:21PT

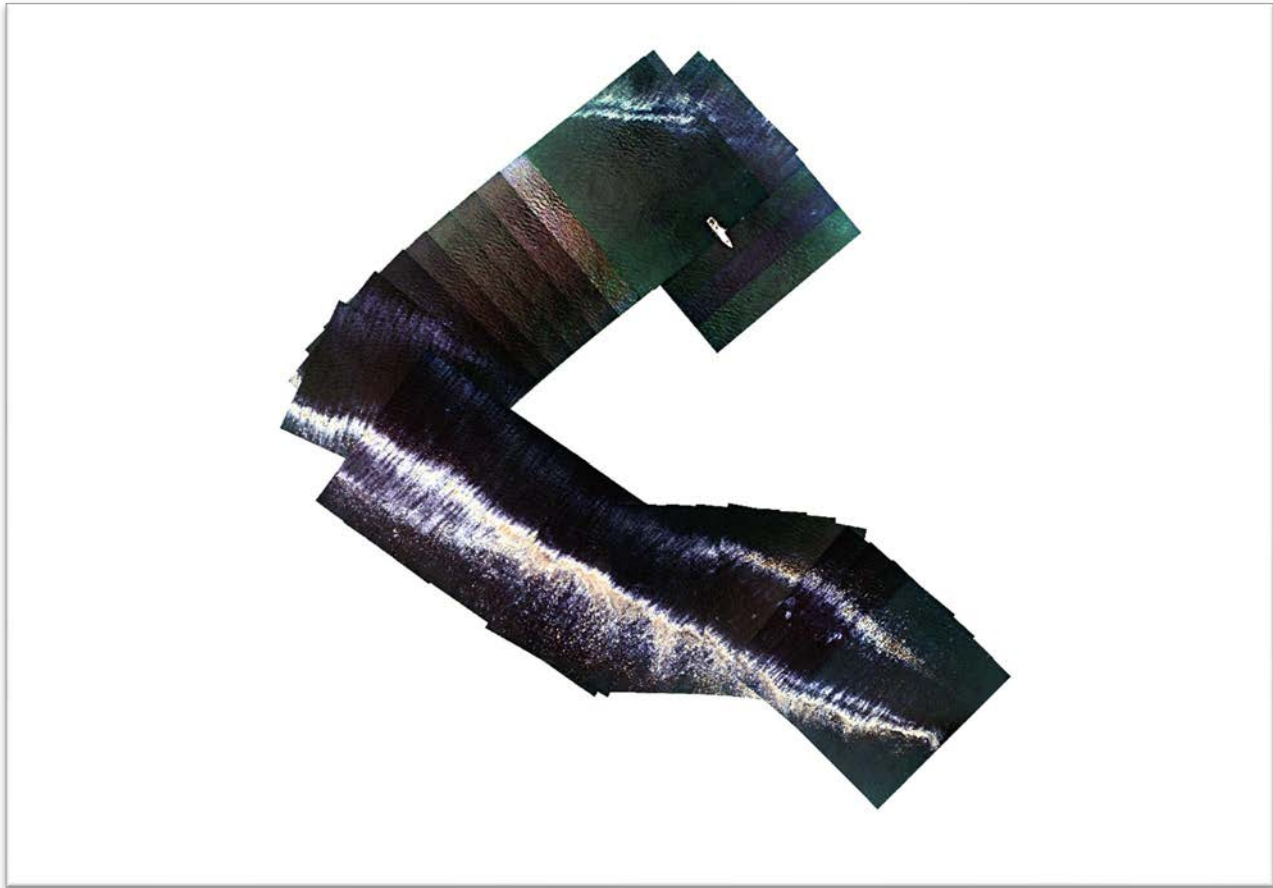


Figure 29. WM_UAS_0512_1354Survey7, collected on May 12 at 13:54PT

The field work on May of 2021 helped us to confirm the processes for rapid generation of the orthomosaics, this process was carried out in less than 10 minutes for each of the surveys. The expedition of this process allowed us to confirm that we could process data in near real time that would show the imagery of the oil as collected from an UAS in near real time. Our next step was to implement the rapid processing of the classification routines. We practiced with the data collected for the surveys shown in Figures 26-29 and were able to generate classification outputs in less than 10 minutes for each of them.

6.2 Huntington Beach Pipeline Oil Spill Incident.

On October of 2021, an oil spill was reported on the coast of the state of California. This spill was named as the Huntington Beach Pipeline Oil spill incident. We were informed about this spill and were asked by NOAA to join the effort of responders to monitor the spill. We mobilized on October 5 and arrived on scene the next day. We used a boat of opportunity to monitor and look for the oil as reports from high altitude airplanes and satellites reported on the previous day that oil was still visible.

On October 6, early in the morning we departed from the harbor of Huntington Beach aboard of a vessel ready to monitor for oil spill. After many hours of transit, we finally spotted the floating layer of oil using our UAS and proceeded to conduct recognizance missions. The aspect of the slick was a thin silver sheen that extended for miles. We were in constant communication via radio and cellphone with the Incident Command and personnel from NOAA. They were receiving constant reports of the thin slick and no sights of thick actionable oil (Figure 30).



Figure 30. UAS aerial view of the oil spill from the Huntington Beach spill incident.

Eventually we were able to find thick actionable, in a very opportunistic way, we reported immediately our location to the Incident Command and proceeded to deploy our UAS system. After retrieving the UAS we use our rapid processing algorithm to process the data collected and produced a map of the actionable oil in less than 20 minutes. This map was immediately distributed to the Incident Command and NOAA colleagues directly through email, and this operation resulted on a successful performance of our system as it was put in practice on a real case where timing was crucial.

Figure 31 shows a map of the oil spill with responder vessels that arrived on scene and were ready to contain the oil. This map was produced in less than 20 minutes after the UAS was retrieved. These maps were distributed to BSEE's manager Dr. Jay Cho at the same time as NOAA and the Incident Command directly from the vessel as we continued the monitoring operations. This exceptional opportunity demonstrated the performance of our system on near-real time, on a real case, and the benefit of having the capacity to report imagery and classification maps so quickly.

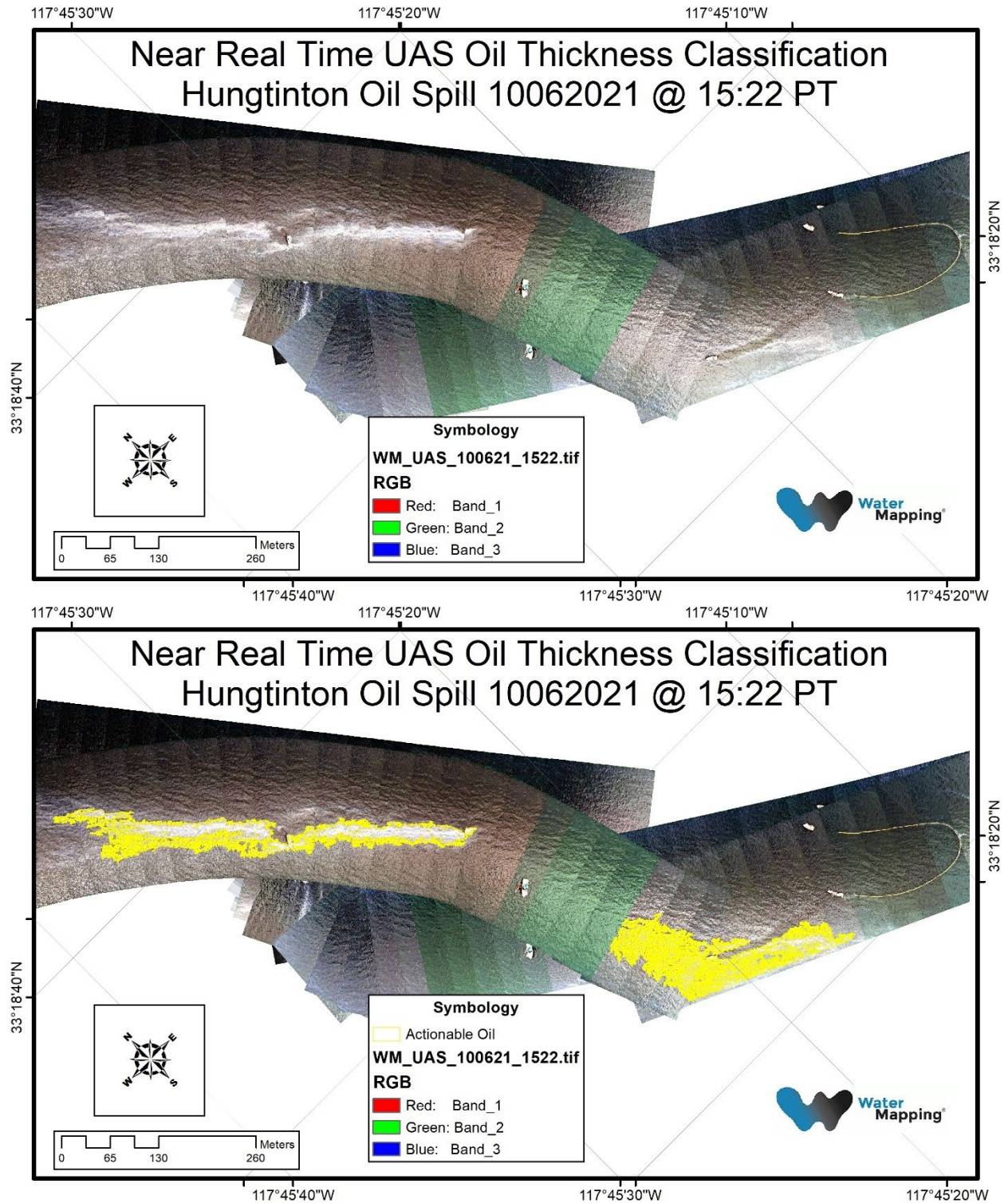


Figure 31. Near real time maps of the oil spill observed during the Huntington Beach spill.

6.3 Oil spill monitoring during NASA-ROSES campaign.

After the Huntington Spill Incident, during the same month of October, we participated with colleagues from NASA and NOAA on a parallel project in which the mission was to collect oil spill thickness maps for the calibration of data processing routines of L-Band SAR data in this case collected by the UAVSAR. This campaign was conducted from October 27 to 29 on board of the USCG blackfin (Figure 32).



Figure 32. USCG Blackfin with its crew on deck including Ben Holt from JPL, Frank Monaldo from NOAA, and Oscar Garcia from Water Mapping, LLC.

This campaign was very successful in part for the weather conditions and the amount of oil observed from the UAS. Next series of figures are some of the snapshots collected by the UAS.



Figure 33. Thick actionable oil is observed from the UAS on October 27.



Figure 34. Thick actionable oil is observed from the UAS on October 28.

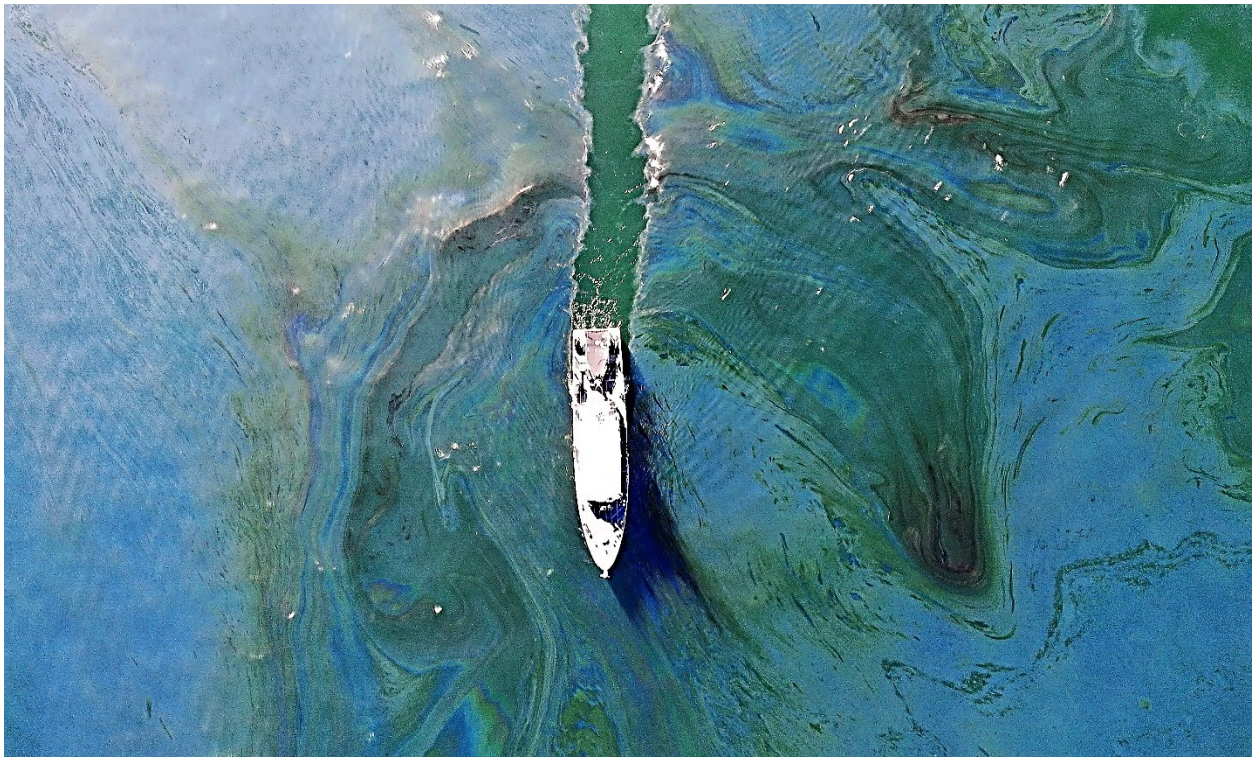
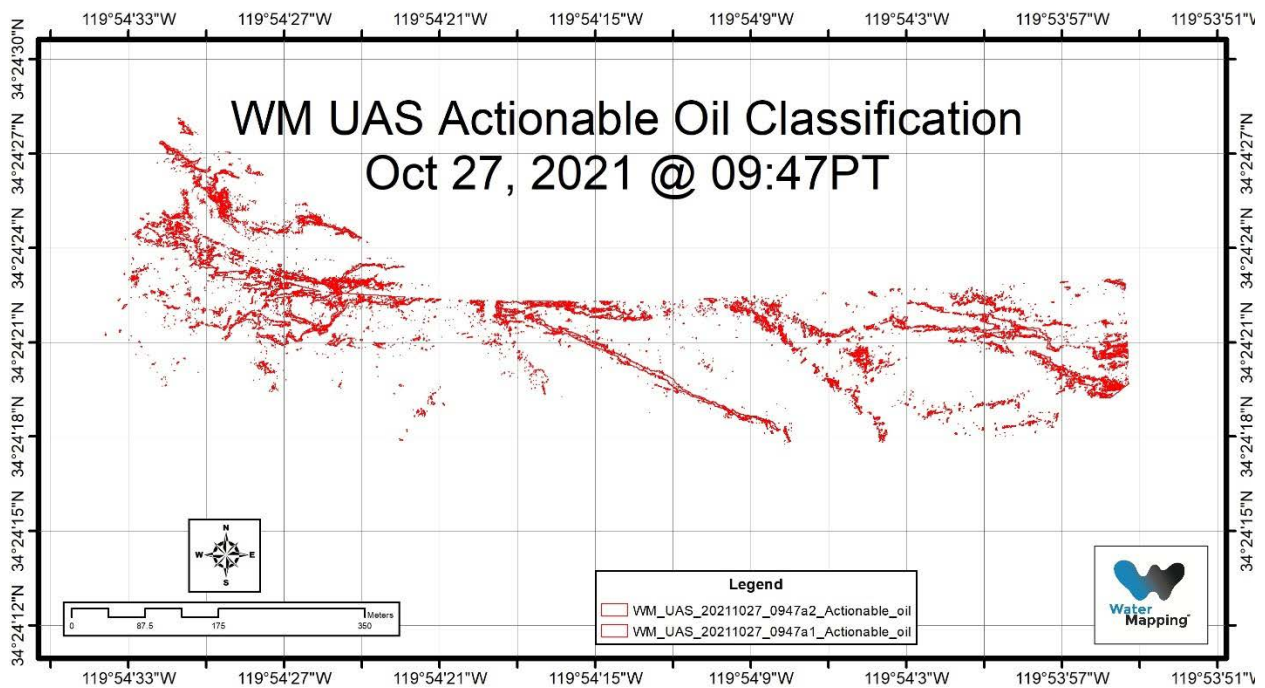
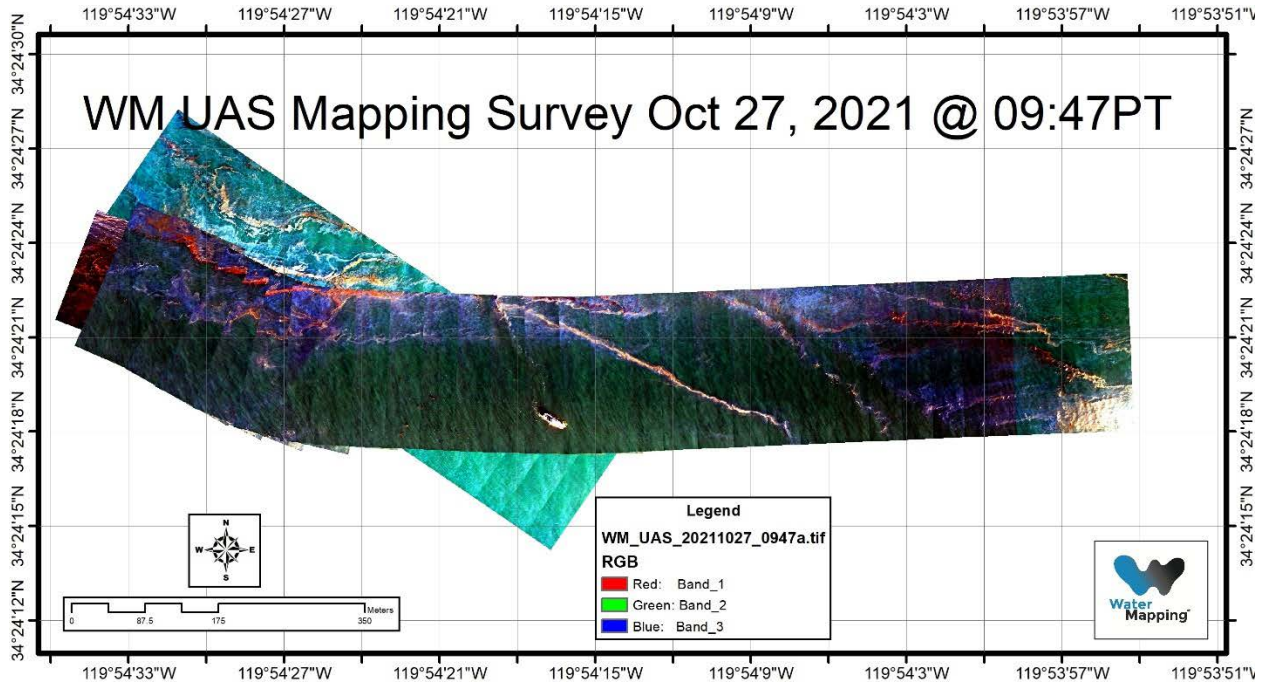
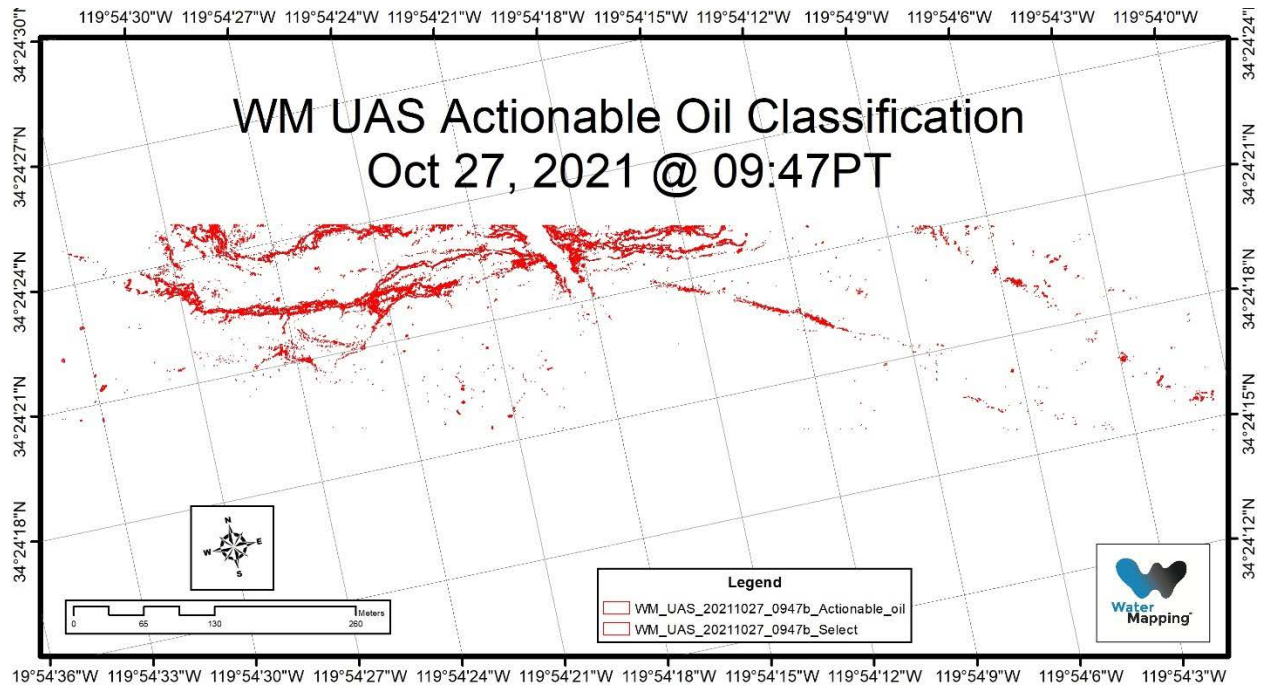
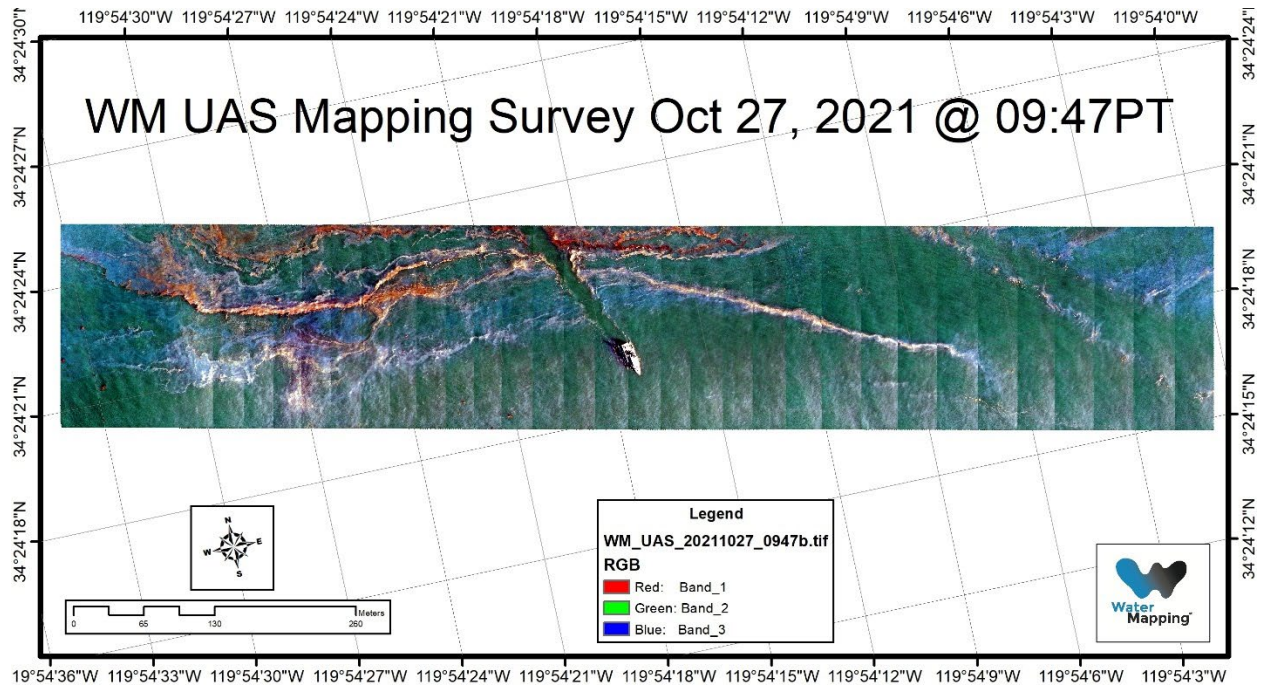
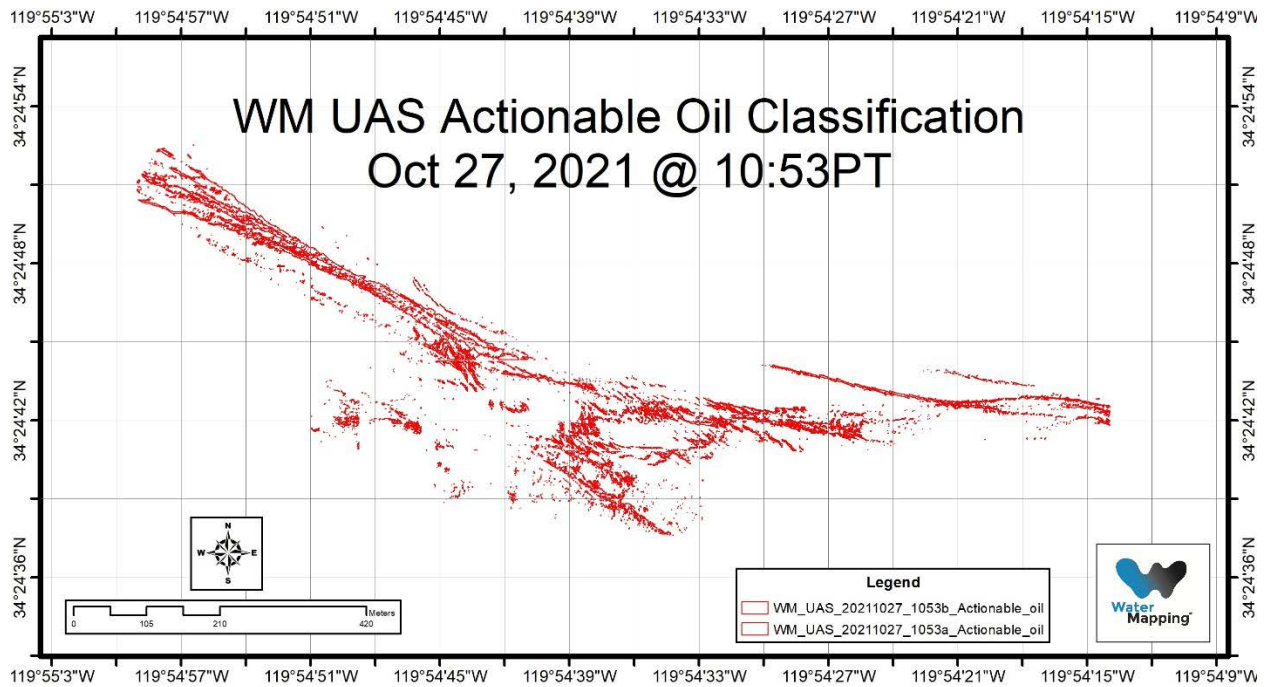
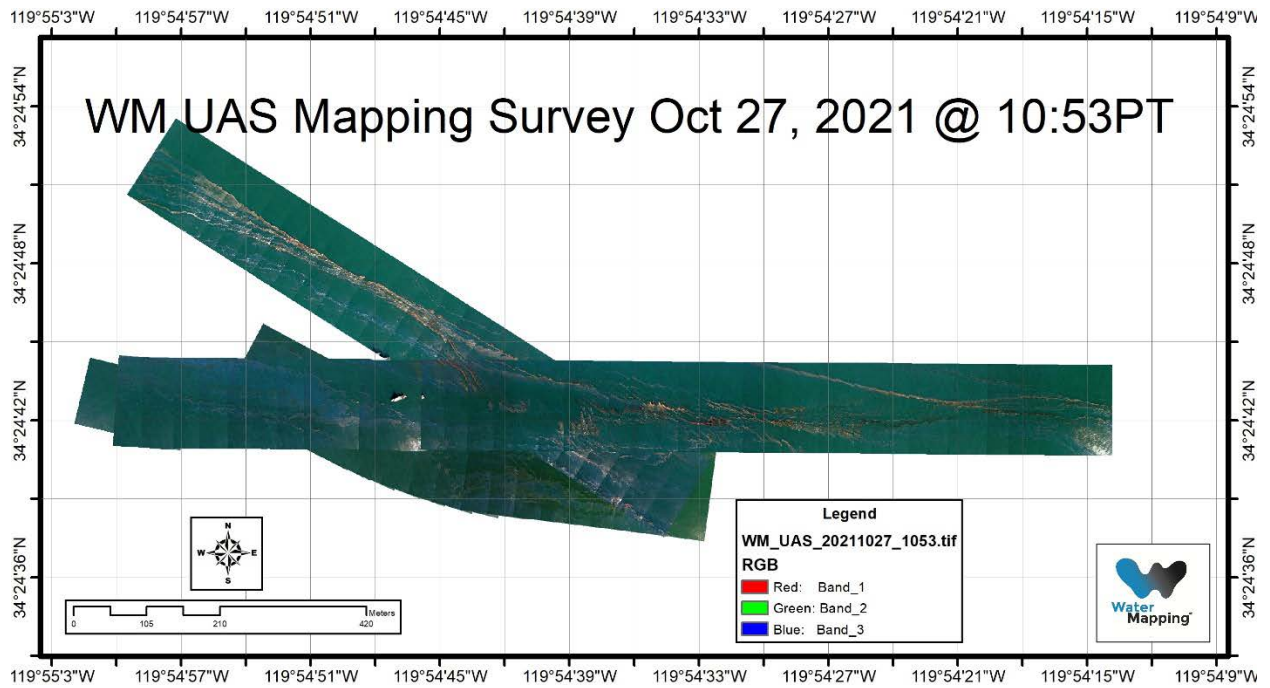


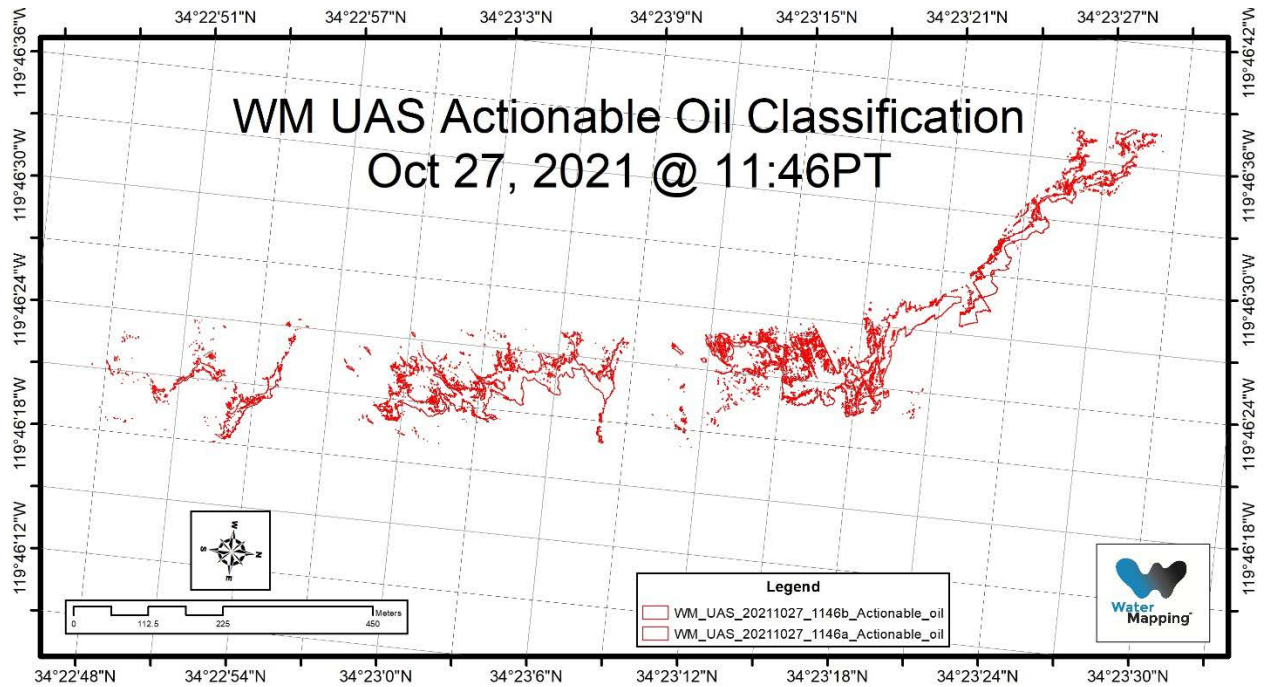
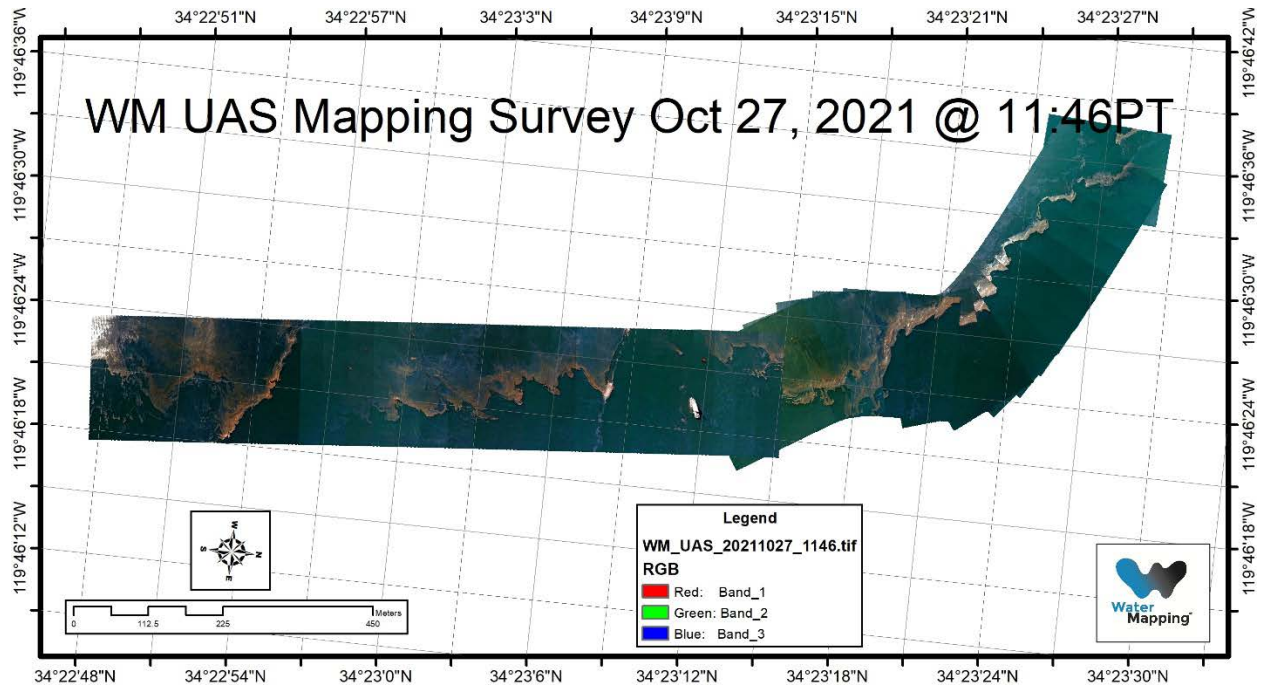
Figure 35. Thick actionable oil is observed from the UAS on October 29.

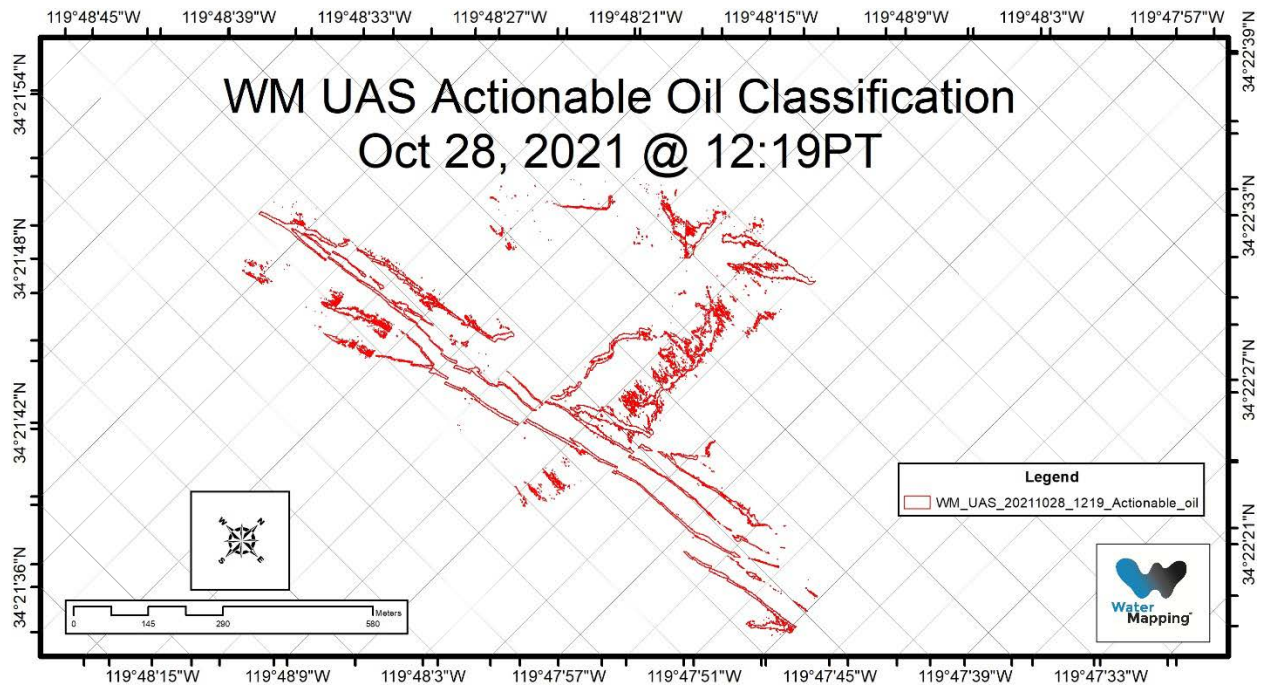
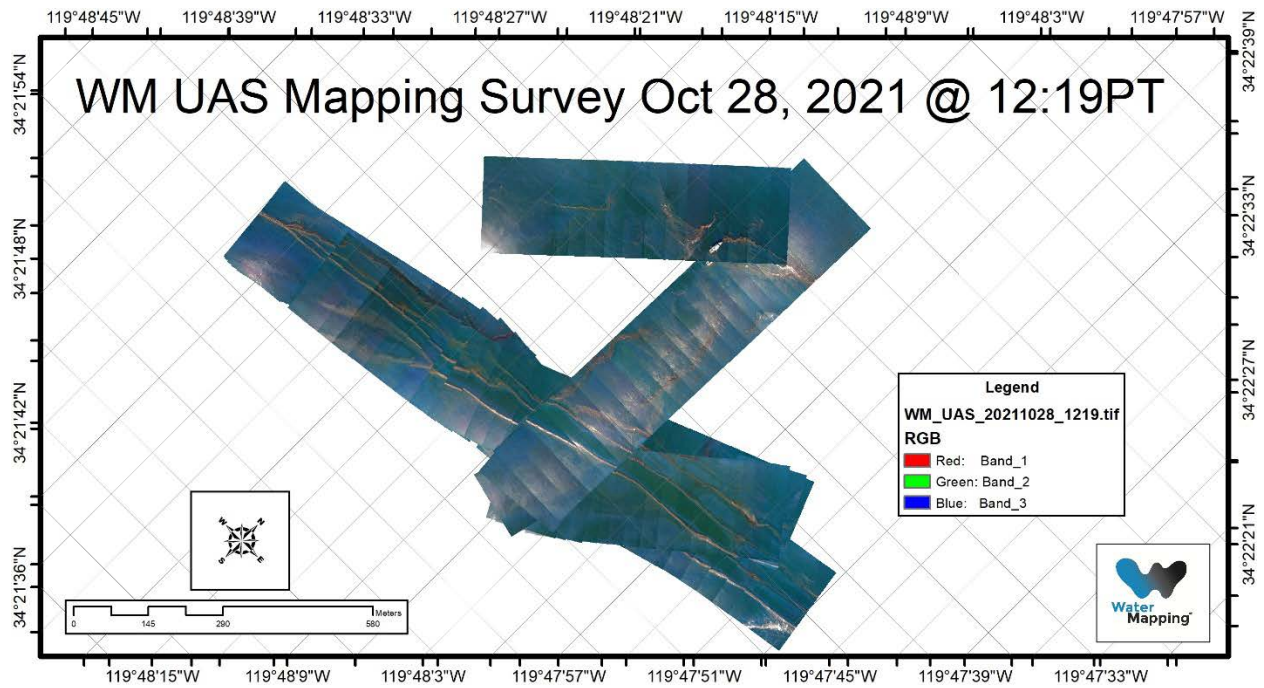
6.4 Near Real time mapping during NASA-ROSES campaign.

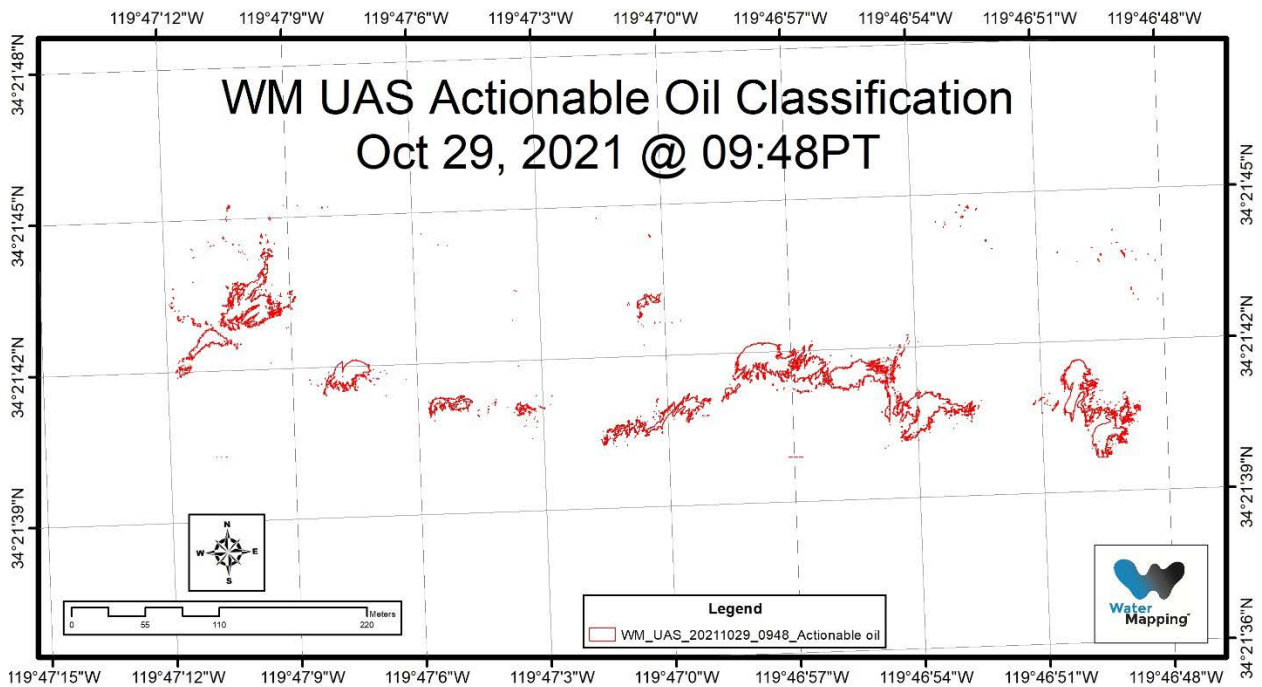
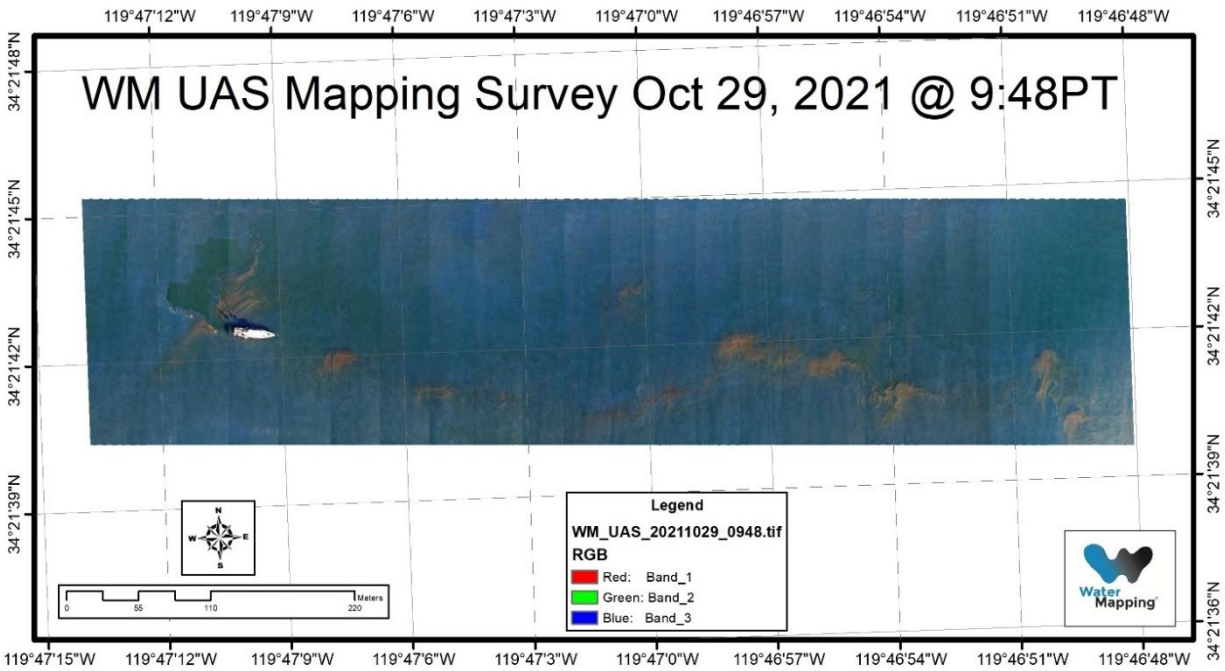


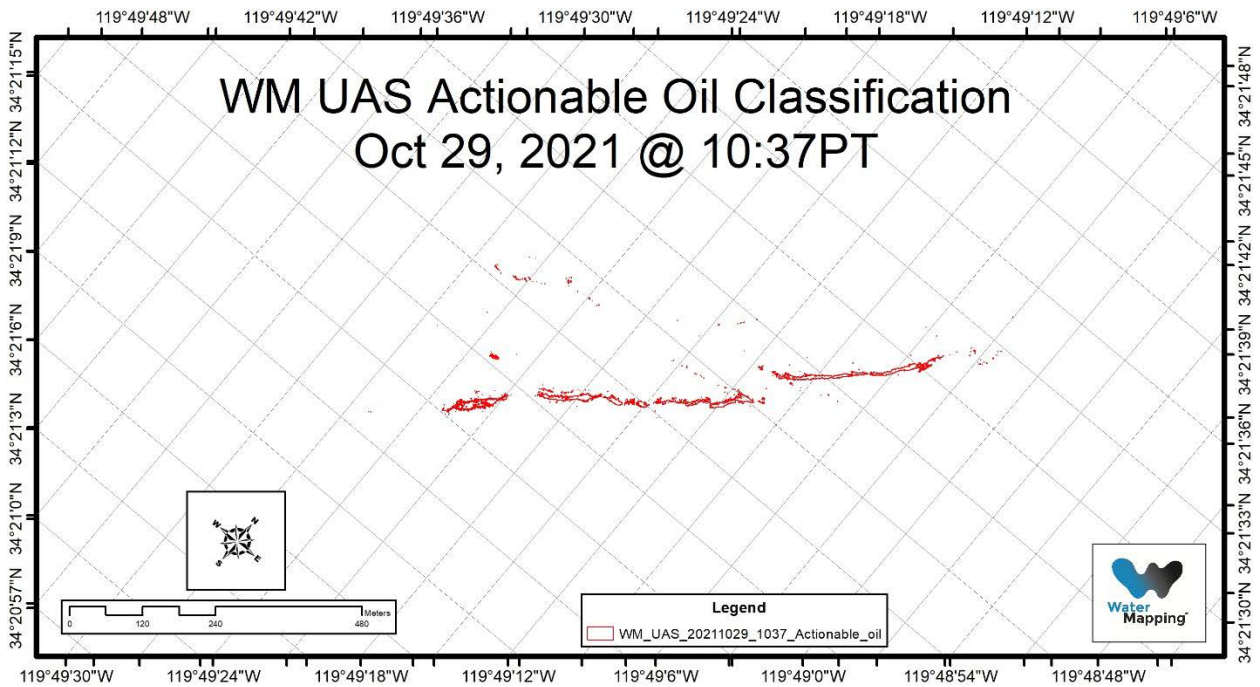
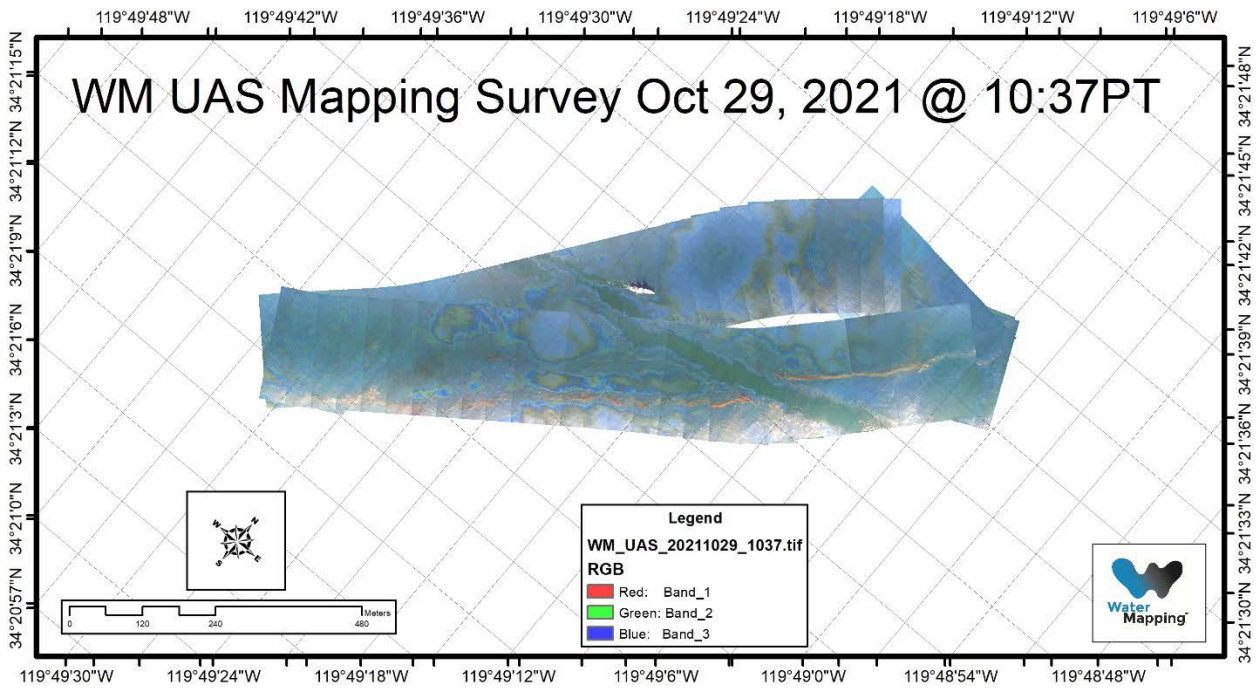


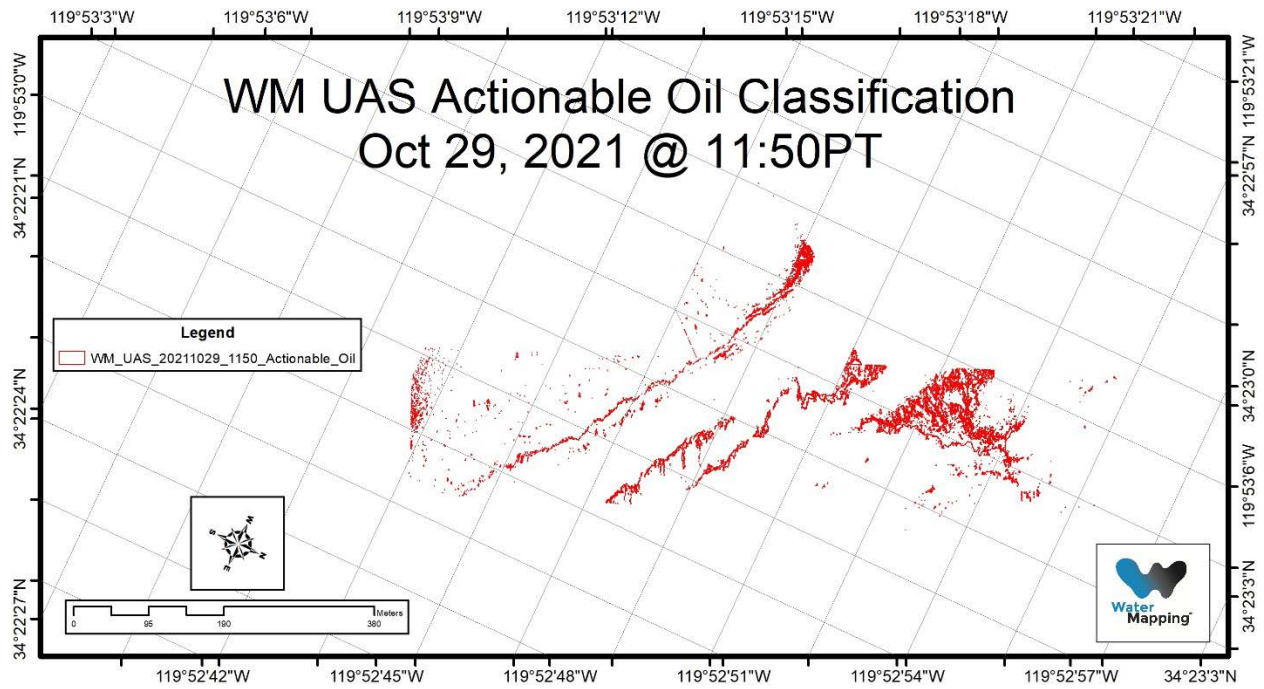
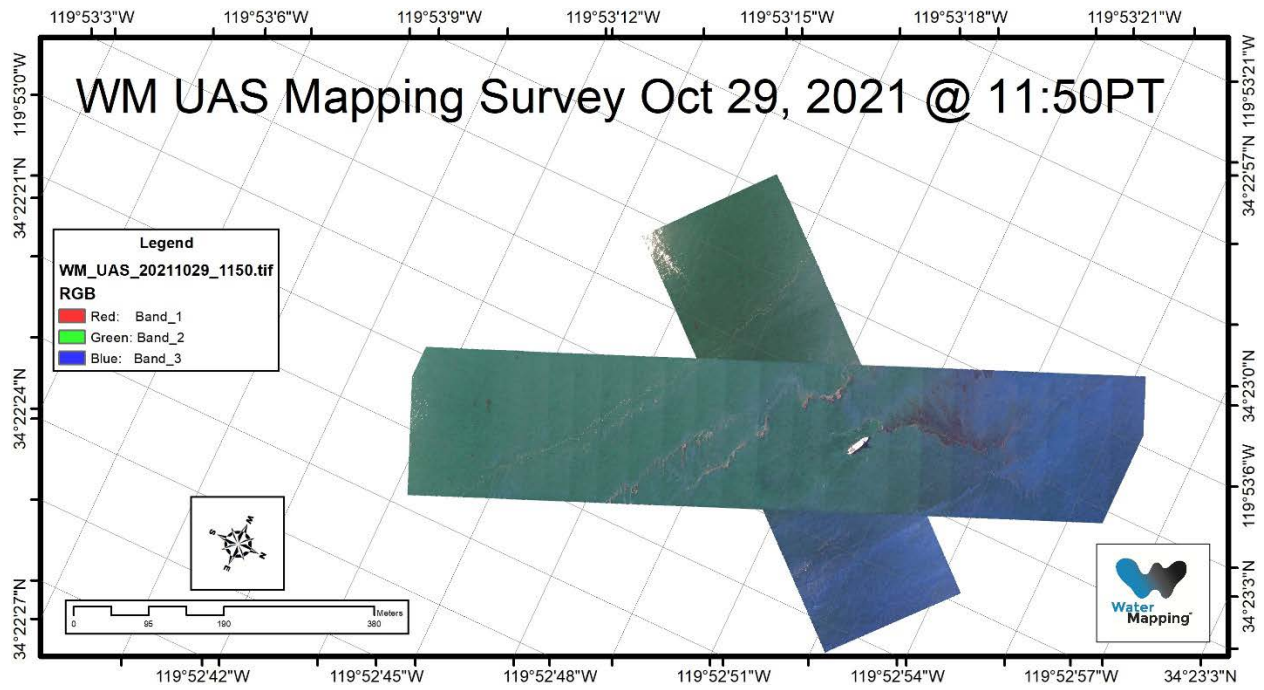


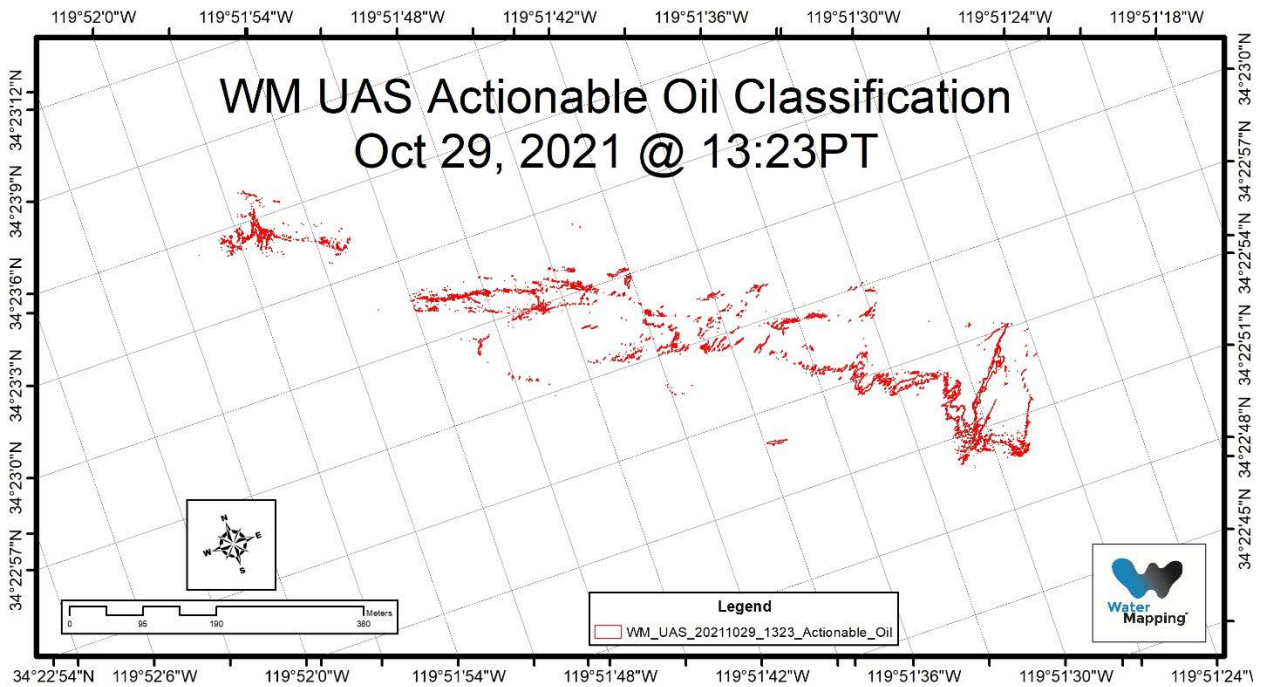
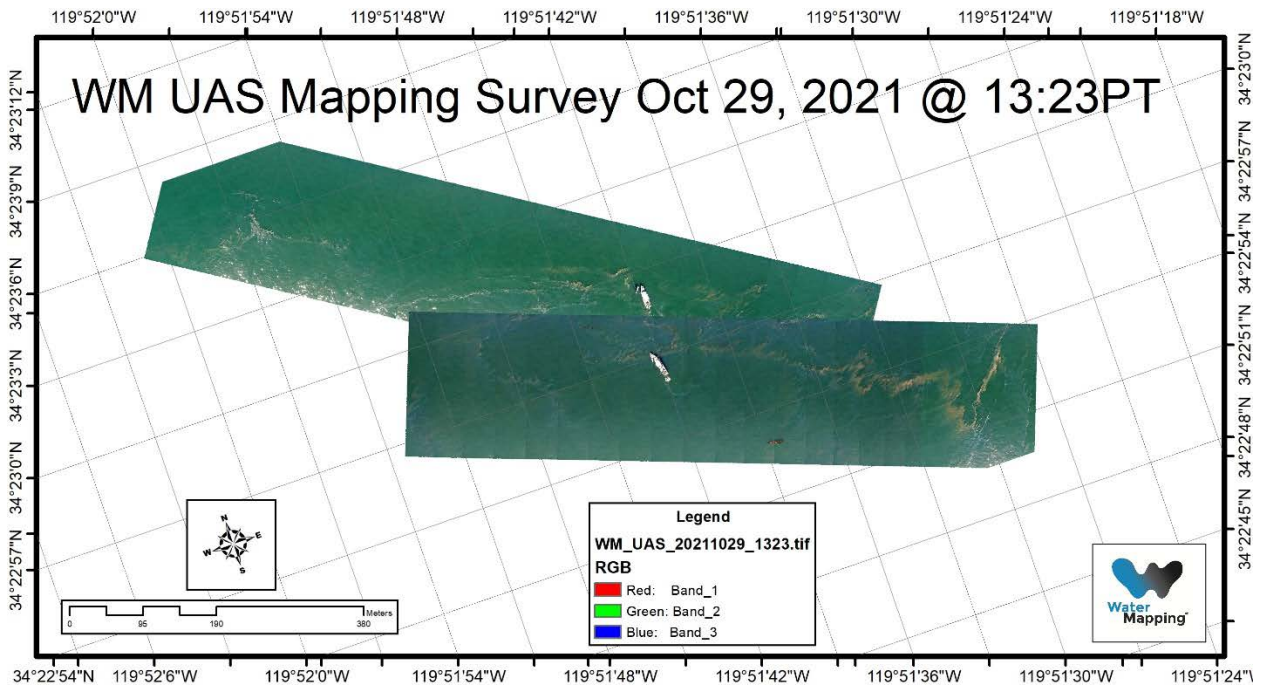












8. Conclusions

We have achieved our goal for producing near real time mapping information for oil spill responders. The system developed to produce near-real time classification maps of floating oil spills is the result of integrating science and elaborated software engineering. As a result of this work, the algorithm/sensor system is capable of identifying areas and locations of actionable oils in real-time for tactical positioning and near-real time (within under 20 minutes from being collected) for response planning. The information generated from the UAS system is compatible with The Environmental Response Management Application, (ERMA®) which will be available to responders in real and near-real time.

We had the opportunity of testing this system on a real setting environment at the Santa Barbara seeps during a couple of field test in May and September of 2021. Then in October of 2021 a spill of opportunity occurred in the coast of the state of California named “Huntington Beach pipeline spill” in which we used this system to demonstrate on a real spill case the usefulness of the near real time system. During this spill we deployed our UAS system and assisted the response delivering near real time maps of the oil spill to the incident command, which helped directing the responders to the site of the detections. This successful story was later repeated as we supported an adjacent project supported by NASA producing a large number of maps of detections to support the calibration of a high altitude aerial sensor called UAVSAR.

Future work will be focused on developing a system that integrates new sensors and that will deliver data in real time.



Department of the Interior (DOI)

The Department of the Interior protects and manages the Nation's natural resources and cultural heritage; provides scientific and other information about those resources; and honors the Nation's trust responsibilities or special commitments to American Indians, Alaska Natives, and affiliated island communities.



Bureau of Safety and Environmental Enforcement (BSEE)

The mission of the Bureau of Safety and Environmental Enforcement (BSEE) works to promote safety, protect the environment, and conserve resources offshore through vigorous regulatory oversight and enforcement.

BSEE Response Research Branch Program

The Response Research Branch (RRB) oversees the Oil Spill Response Research Program (OSRR) and manages the National Oil Spill Response and Renewable Energy Test Facility (Ohmsett). The research conducted under OSRR aims to improve oil spill response and preparedness by advancing the state of science and the technology used in responding to offshore oil spills. The research also supports the Bureau's needs while ensuring the highest level of scientific integrity by adhering to BSEE's peer review protocols. The proposal, selection, research, review, collaboration, production, and dissemination of each of BSEE's Response Research Branch Program follows the DOI Code of Scientific and Scholarly Conduct, in support of a culture of scientific and professional integrity, as set out in the DOI Departmental Manual (305 DM 3).